AD-A154 967 SOLAR CYCLE VARIATION OF EPHEMERAL REGIONS(U) NATIONAL OCEANIC AND ATMOSPHERIC ADMINISTRATION BOULDER CO K L HARVEY 01 DEC 84 AFGL-TR-84-0335 ESD-84-611 1/1

UNCLASSIFIED F/G 3/2 NL

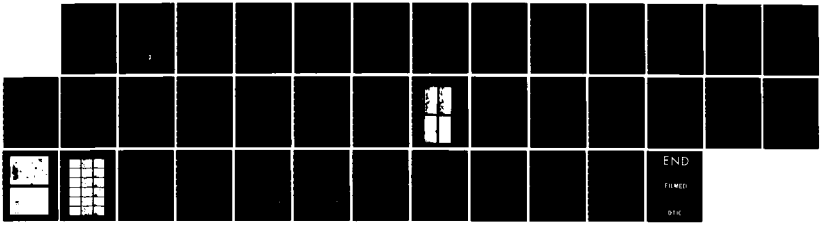

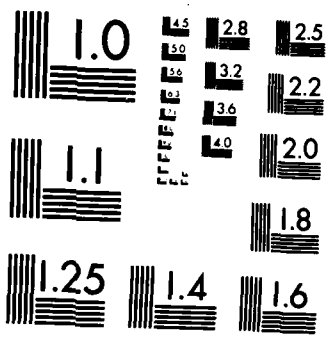

AFGL-TR-84-0335

SOLAR CYCLE VARIATION OF EPHEMERAL REGIONS

Karen L. Harvey

National Oceanic and Atmospheric Administration
325 Broadway
Boulder, Colorado 80303

1 December 1984

Final Report
1 November 1983 - 1 November 1984

Approved for public release; distribution unlimited

AIR FORCE GEOPHYSICS LABORATORY
AIR FORCE SYSTEMS COMMAND
UNITED STATES AIR FORCE
HANSCOM AFB, MASSACHUSETTS 01731

This report has been reviewed by the ESD Public Affairs Office (PA) and is releasable to the National Technical Information Service (NTIS).

This technical report has been reviewed and is approved for publication.

Richard C. Altrock
Contract Manager

STEPHEN L. KEIL
Branch Chief

FOR THE COMMANDER

RITA C. SAGALYN

Division Director

Qualified requestors may obtain additional copies from the Defense Technical Information Center. All others should apply to the National Technical Information Service.

If your address has changed, or if you wish to be removed from the mailing list, or if the addressee is no longer employed by your organization, please notify AFGL/DAA, Hanscom AFB, MA 01731. This will assist us in maintaining a current mailing list.

Do not return copies of this report unless contractual obligations or notices on a specific document require that it be returned.

Unclassified

SECURITY CLASSIFICATION OF THIS PAGE

REPORT DOCUMENTATION PAGE

1a. REPORT SECURITY CLASSIFICATION: Unclassified	1b. RESTRICTIVE MARKINGS
2a. SECURITY CLASSIFICATION AUTHORITY	3. DISTRIBUTION/AVAILABILITY OF REPORT: Approved for public release; distribution unlimited
2b. DECLASSIFICATION/DOWNGRADING SCHEDULE	
4. PERFORMING ORGANIZATION REPORT NUMBER(S)	5. MONITORING ORGANIZATION REPORT NUMBER(S): AFGL-TR-84-0335
6a. NAME OF PERFORMING ORGANIZATION: National Oceanic and Atmospheric Adm (NOAA) / 6b. OFFICE SYMBOL (If applicable)	7a. NAME OF MONITORING ORGANIZATION
6c. ADDRESS (City, State and ZIP Code): 325 Broadway, Boulder Colorado 80303	7b. ADDRESS (City, State and ZIP Code)
8a. NAME OF FUNDING/SPONSORING ORGANIZATION: Air Force Geophysics Laboratory / 8b. OFFICE SYMBOL (If applicable): PHS	9. PROCUREMENT INSTRUMENT IDENTIFICATION NUMBER: ESD 84-611
8c. ADDRESS (City, State and ZIP Code): Hanscom AFB, Massachusetts 01731	10. SOURCE OF FUNDING NOS.

PROGRAM ELEMENT NO.	PROJECT NO.	TASK NO.	WORK UNIT NO.
61102F	2311	G3	CX

11. TITLE (Include Security Classification): Solar Cycle Variation of Ephemeral Regions

12. PERSONAL AUTHOR(S): Karen L. Harvey *

13a. TYPE OF REPORT	13b. TIME COVERED	14. DATE OF REPORT (Yr., Mo., Day)	15. PAGE COUNT
Final Report	FROM 1 Nov 83 TO 1 Nov 84	1 December 1984	35

16. SUPPLEMENTARY NOTATION

*Solar Physics Research Corporation, Tucson, AZ

17 COSATI CODES			18. SUBJECT TERMS (Continue on reverse if necessary and identify by block number)
FIELD	GROUP	SUB GR.	Solar observations Solar X-rays Helium

19. ABSTRACT (Continue on reverse if necessary and identify by block number)

Ephemeral active regions (ER) have been identified and counted for selected periods from 1970 to mid-1984 using the daily, full-disk photospheric magnetograms taken by the National Solar Observatory. The number of ephemeral regions varies nearly in phase with the solar cycle. At solar minimum, ER are distributed almost uniformly in latitude; by solar maximum, peaks in the latitude distribution are observed in the sunspot zones and in higher latitude bands. In the quiet sun, 37% of the He I λ10830 'dark points', used as a proxy for X-ray bright points (XBP), are associated with ER; 63% overlie bipoles that appear to be the chance encounter of opposite polarity network. The percentages are somewhat different in coronal holes; 21% of the dark points in He I are associated with ephemeral regions and 79% with bipoles that apparently result from chance encounters of flux. The dark points observed in the quiet sun and in coronal holes, vary anti-correlated with the solar cycle. Little relations was found between the areal density of He I dark points and ephemeral regions within the boundaries of coronal holes and parameters of the high speed solar wind streams associated with coronal

20. DISTRIBUTION/AVAILABILITY OF ABSTRACT	21. ABSTRACT SECURITY CLASSIFICATION
UNCLASSIFIED/UNLIMITED ☐ SAME AS RPT ☒ OTIC USERS ☐	Unclassified

22a. NAME OF RESPONSIBLE INDIVIDUAL	22b. TELEPHONE NUMBER (Include Area Code)	22c. OFFICE SYMBOL
R. Altrock		PHS

DD FORM 1473, 83 APR EDITION OF 1 JAN 73 IS OBSOLETE

SECURITY CLASSIFICATION OF THIS PAGE

Block 19 Contd

holes.

This study suggests that (1) ephemeral regions are not small active regions and that they may be primarily a surface phenomena, possibly resulting from convection interacting with sub-photospheric fields, and (2) He I 'dark points,' and therefore, XBP, are more often associated with the encounter of existing opposite polarity network flux, the occurrence of which is related to the amount of mixed polarity areas which varies inversely with the solar cycle.

SOLAR CYCLE VARIATION OF EPHEMERAL REGIONS

Karen L. Harvey

Solar Physics Research Corporation, Tucson, AZ, USA

Abstract: Ephemeral active regions (ER) have been identified and counted for selected periods from 1970 to mid-1984 using the daily, full-disk photospheric magnetograms taken by the National Solar Observatory. The number of ephemeral regions varies nearly in phase with the solar cycle. At solar minimum, ER are distributed almost uniformly in latitude; by solar maximum, peaks in the latitude distribution are observed in the sunspot zones and in higher latitude bands. In the quiet sun, 37% of the He I λ10830 'dark points', used as a proxy for X-ray bright points (XBP), are associated with ER; 63% overlie bipoles that appear to be the chance encounter of opposite polarity network. The percentages are somewhat different in coronal holes; 23% of the dark points in He I are associated with ephemeral regions and 77% with bipoles that apparently result from chance encounters of flux. The dark points observed in the quiet sun and in coronal holes, vary anti-correlated with the solar cycle. A relation is suggested between parameters of the high speed solar wind streams associated with coronal holes and the coronal hole areal density of He I dark points for the entire data sample and with ephemeral regions in coronal holes during the few year period around sunspot minimum.

This study suggests that (1) ephemeral regions are not small active regions and that they may be primarily a surface phenomena, possibly resulting from convection interacting with sub-photospheric fields, (2) He I 'dark points', and therefore, XBP, are more often associated with the encounter of existing opposite polarity network flux, the occurrence of which is related to the amount of mixed polarity areas which varies inversely with the solar cycle, and (3) there is some correlation of the areal density of dark points and ephemeral regions with parameters of the high speed solar wind streams associated with coronal holes. This relation appear to be a function of the solar cycle.

1. Introduction

Ephemeral regions (ER) are small scale bipolar regions of characteristic size of 10^4 km, an average total magnetic flux of 3.3×10^{19} Mx and lifetimes ≤ 1 day. Based on magnetic field data from 1970 to 1975, previous studies (Harvey *et al.*, 1975; Harvey and Harvey, 1976; Martin and Harvey, 1979) indicate that hundreds of ER emerge on the Sun per day and that the number of ER varies nearly in phase with the solar cycle. Ephemeral regions also have been identified with soft X-ray and EUV bright points (Golub *et al.*, 1974, 1977), bright coronal structures having about the same size, lifetime, latitude distribution and behavior as ER. The variation of the coronal bright points, however, is 180° out of phase with the solar cycle (Davis *et al.*, 1977; Golub *et al.*, 1979; Golub, 1980; Davis, 1983).

In the study presented in this report, the global properties of ephemeral regions over the solar cycle and their association with He I λ10830 dark points (that correspond to X-ray/EUV bright points) have been re-examined using a data set covering almost the entire current solar cycle.

2. Data

The data used are the daily full disk observations of the longitudinal photospheric fields (Fe I λ8688) and He I λ10830 spectroheliograms taken by the National Solar Observatory. Magnetograms have been obtained since 1970 but only on a systematic basis since 1973. From 1970-1973 these data were taken with a 40-channel magnetograph (Livingston *et al.*, 1971) using the main image at the McMath Telescope; spatial resolution of these data is 2.5 arc-sec. Subsequent magnetic field observations and the He I spectroheliograms with spatial resolution of 1 arc-sec. were obtained using the 512-channel magnetograph (Livingston *et al.*, 1976) at the Vacuum Telescope located on Kitt Peak.

For each year from 1970 through 1984, three to five 7 to 20 day periods of continuous good quality observations were selected for analysis. Ephemeral regions were identified by an overlay of two successive daily magnetograms and an assessment of the probability of small-scale bipolar structures being a new region or the 'chance' encounter of existing opposite polarity network elements. An example is shown in Figure 1 for a section of the full disk magnetograms on 9 and 10 August 1978. The boxes indicate the identifications on 10 August of newly emerged bipoles (that are not observed on the previous day and could not be explained by the migration of existing magnetic flux); the arrowheads designate the locations of 'chance' encounters of opposite polarity network (i.e., bipoles that might be explained by the migration and encounter of flux existing on the previous day). For two of the selected periods each year, the positions and lifetimes of identified ER were measured. From the ER positions, a visibility function, i.e., how well new ER can be detected as a function of distance from the Sun's center, was empirically determined assuming that (1) the number of ER within 25° of the equator are distributed uniformly in longitude, and (2) the visibility function could be expressed as $\cos^n \theta$. This function was used to correct the counts of ephemeral regions and their spatial distributions. Errors in the counts and positional distributions were estimated by dividing the data into two subsets.

3. Global Properties of Ephemeral Regions

3.1. SOLAR CYCLE VARIATION

The number of ephemeral regions observed on the Sun at any given time from 1970 to 1984 is shown in Figure 2. Their temporal variation has been compared in Figure 2a with the sunspot numbers (R_z), determined for the same intervals for which ER counts were made and in Figure 2b with the Sun's total magnetic flux, determined from the daily NSO magnetograms. The graph shows that the number of ER varies nearly in phase with the solar cycle, confirming our earlier results (Martin and Harvey, 1979). A minimum in ephemeral region counts occurred in early 1975 more than one year before sunspot minimum, again consistent with previous results (Martin and Harvey, 1979). The ER minimum, however, does occur at the time of a minimum in the Sun's total magnetic flux (Figure 2b). From minimum (1975) to maximum (1979-81) the number of ER doubled. In comparison, the total flux on the Sun increased by a factor of 3.5 (J. Harvey, private communication) and sunspot numbers increased by a factor of 38.

The total number of ephemeral regions that emerged during the period covered by this analysis can be estimated by integrating under the time variation curve of ER shown. Assuming the average ER lifetime is 12 hours, the total number of ER that have emerged from 1973-1984 (equivalent to one solar cycle) is 4.5×10^6; if the average lifetime is 18 hours (the e-folding time based on the lifetime distribution discussed in §3.3), the total number of ER is 3.0×10^6. Tang *et al.* (1984) find that the integral number of active

regions of a given size and larger decreases exponentially with increasing region size (Figure 3). If ER are small active regions, their results suggest there should be $\sim 2 \times 10^3$ ER; this is a factor of $1.5\text{-}2.3 \times 10^3$ less than is estimated on the basis of the observed number of ER.

3.2. LATITUDE DISTRIBUTION

The distribution of ER in latitude shows that these regions occur over the entire surface of the Sun and that their distribution changes with the development of the solar activity cycle. In Figure 4, the distribution of observed ER has been plotted for three phases of the solar cycle. A uniform distribution determined by applying the visibility function to the average ER count between $\pm .1$ sine latitude also has been plotted. During sunspot minimum (1975-76), ephemeral regions appear to be almost uniformly distributed in latitude. By 1979-1980, their latitude variation shows an increase in the sunspot zones and in the latitude belts centered around $\pm 30^\circ$ and $\pm 50^\circ$. As the cycle declines, there is a trend toward a more uniform distribution by 1983-84 with the peaks at solar maximum still evident but of smaller magnitude.

3.3. LIFETIMES OF ER

The lifetime distribution for ephemeral regions, shown in Table I, was determined by the number of sequential magnetograms on which an ER was detected. Ephemeral regions seen on only one magnetogram have a lifetime of less than 2 days and seen on two magnetograms a lifetime of 1-3 days, etc.

Table I

Lifetime Distribution of Ephemeral Regions

	% of Ephemeral Regions						
Year	1 mg*	2 mgs	3 mgs	4 mgs	5 mgs	6 mgs	Total ER
1975	67.3	24.6	5.7	2.2	0.3	0.0	761
1976	83.4	12.4	3.6	0.6	0.0	0.0	884
1977	78.8	15.2	5.1	0.7	0.0	0.2	1043
1979	70.6	18.8	8.2	0.9	1.2	0.4	1652
1980	70.4	19.9	5.9	3.2	0.5	0.1	1460
1981	73.2	18.4	5.9	2.2	0.3	0.1	1614
1983-4	70.2	23.8	4.6	0.9	0.5	0.0	1421
1975-84	73.4	19.0	5.6	1.5	0.4	0.1	8835
Lifetime** (days)	>0-<2	1-<3	2-<4	3-<5	4-<6	5-<7	

* number of magnetograms

**range in lifetime

The decay of the population of ER for the data sample from 1975-1984 follows the exponential curve $N = A \times e^{-t/\tau}$, where N is the number of ER, A=274.3 ± 5.7, t is the lifetime in days and $\tau = 0.76 \pm 0.01$. The correlation coefficient between the number of ER and their lifetime is 0.9998.

4. Association of ER with He I λ10830 'Dark Points'

Other than during the Skylab period (1973), no time sequence imaging of the Sun in soft X-rays has been available to study simultaneously the evolution of XBP and ER. A possible avenue to study this problem in lieu of soft X-ray images of the Sun is suggested by the results of Harvey *et al.* (1975). They found that X-ray bright points (XBP) correspond to similar sized but dark structures in He I D_3 and in He I λ10830. The 'dark points' observed in He I λ10830 are thought to result from the EUV/X-ray emission ($\lambda < 500$ Å) in the corona (coronal bright point) exciting the underlying chromospheric He I. This observed correlation provides a tool to consider the association of ER with XBP both as a function the solar cycle and their evolution.

The daily He I λ10830 spectroheliograms were analyzed from 1975-1984 for the two selected periods of each year within a radius vector of ≤ 0.4 from the Sun's center. This distance restriction allowed the more accurate determination of the characteristics of the underlying magnetic field without significant geometric effects entering into the results. He I structures were selected as 'dark points' if their intensity was darker (by 10-15%) relative to the surrounding network and their size was 5-30 arc-sec. In comparing the locations of the He I dark points with the magnetic field observations, 13% were found to occur in a filament channel and are possibly small fragment of filament or they were co-spatial with unipolar network (though a new bipole may have emerged in the approximately 1-1.5 hour period between the magnetic field and He I observation). 87% of the identified He I 'dark points' were associated with small bipoles. 37% of these were at the locations of ephemeral regions; this is somewhat less than the ~50% overlap found between XBP and ER by Golub *et al.* (1977) and considerably less than the 100% association found by Tang *et al.* (1982) for a small sample (2) of bright points observed in C IV. The remaining 63% of the dark points observed in λ10830 corresponded with bipolar regions that appear to be the 'chance' encounter of existing network of opposite polarities, such as illustrated in Figure 1.

The number of the He I 'dark points', plotted from 1976 to 1984 in Figure 5, shows a temporal variation similar to the X-ray bright point counts during the rise of the current solar cycle (Figure 6). But, while the decrease in dark point counts is consistent with what has been found for X-ray bright points (Davis, 1983), the magnitude of the decrease from 1976 to 1979-80 in the dark point counts is less than is seen in the X-ray data. This suggests that we may not be detecting or identifying all of the He I structures that correspond to X-ray bright points. This may be due in part to the array of chromospheric structures visible in He I 10830 confusing the identification of these X-ray bright point counterparts and to the fact that no information is available on the details of the evolution of these features. In light of this the question then arises as to how reliable is the result of the predominate association of dark points with identified 'chance' encounters of existing flux. The answer was pursued in three ways: (1) investigating the characteristics of the He I λ10830 structures associated with the sample of ephemeral regions to determine if 'dark points' are being missed, (2) a re-analysis of the identification of ephemeral regions in a comparison of X-ray and magnetic field data in Fig. 1 of Golub *et al.* (1977, p. 114), and (3) the study of a time-sequence set of simultaneously obtained He I λ10830 and photospheric magnetic field data of the quiet sun.

To ascertain if some dark points are being missed (particularly in association with ephemeral regions), the intensity characteristics of the He I λ10830 structures corresponding to ephemeral regions were examined. Five intensity levels were set and determined relative to the surrounding network, as follows: (1) dark point, (2) darker, (3) same, (4) lighter and (5) none. The results are shown in Table II.

Table II

Intensity of ER-Associated He I Structures

Intensity Level	Number of ER	% of ER
dark point	252	16.6%
darker	386	25.5
same	659	43.5
lighter	127	8.4
none	91	6.0

Though the distribution in intensity is skewed toward the darker intensities, 58% of the ephemeral regions have no recognizable structure in He I λ10830 that distinguishes it from the quiet sun network, i.e., the associated He I structures have the same or lighter intensity as the surrounding network. It appears then that in this data many ephemeral regions are not associated with He I dark points or structures and that dark points associated with ER in the quiet sun are not being missed. No similar analysis has been done for He I structures overlying bipoles thought to be 'chance encounters' of flux.

The association of X-ray bright points with 'chance' encounters and ER has also been assessed by re-examining the identification of ephemeral regions made by Golub *et al.*'s (1977, Figure 1, p. 114) . The 40-channel NSO magnetograms from 20 and 21 August 1973 were compared using the same criteria for the identification of ER used earlier in this study. In Figure 7, most of the bipolar regions associated with X-ray bright points are circled in both the X-ray and magnetic field images. Those regions that are considered as 'chance' encounters of existing opposite polarity network are indicated by an adjacent arrow. 44% of the bipolar magnetic structures accompanied by an XBP fall into this category. Those regions without an arrow are identified as ephemeral regions that have emerged since the observation on or before 20 August.

Though no simultaneous observations are available of the evolution of the magnetic bipoles underlying coronal bright points, Golub *et al.* (1977) presented convincing arguments that X-ray bright points were associated with emerging ephemeral regions based on their similar scale, lifetimes, latitude distributions and evolution. In this current study, the identification of a bipole as being an 'chance' encounter of existing network flux rather than newly emerged flux rests on the interpretation of the motions of the pattern of magnetic flux seen on once-per-day magnetograms. To resolve the discrepancy between the results of these two studies requires simultaneous observations of the development and evolution of the magnetic region and the overlying corona. In an effort to accomplish this, observations in an area of the quiet sun were made over a several hour period for three days in October 1983. He I λ10830, used as an X-ray/EUV proxy, were made by the National Solar Observatory's 512-channel magnetograph at the Vacuum Telescope on Kitt Peak; photospheric magnetograms were obtained with the video magnetograph at Big Bear Solar Observatory. Figure 8 shows a section of the data obtained on 11 October 1983 illustrating (1) the development of He I 'dark points' in association with the encounter of apparently unrelated but existing opposite polarity network and (2) the change in He I structures accompanying the emergence of an ephemeral region. In the first case, a negative (black) pole, located in the lower part of the area shown, contracted in area and moved toward the nearby positive pole. Connecting fibrils are obvious in the Hα filtergrams at 2013 UT. By 2056 UT, the two poles are adjacent. Later observations show an apparent weakening of the negative pole. Accompanying the convergence of these two opposite polarity poles is the development of a

dark 'point' in He I 10830 around 1844 UT, positioned between the two poles. Fluctuations in intensity of this He I structure occurred throughout the rest of the observations.

In the upper left quadrant of the area shown in Figure 8, a new small bipolar region first became visible in the magnetic field observations at 1819 UT. During the separation of the emerging region's poles, the positive component merged with network of same polarity. The region's total magnetic flux (Φ) measured at 2143 UT is 3.3×10^{19} Mx, though at this time the region's flux appears to be significantly out of balance (the ratio of Φ_+ to Φ_- is 5). In He I 10830, a minor and short-lived darkening occurred at 1930 UT followed by a flare-like darkening just north of the new region from 2013-2043 UT. At 2111 UT, a more extensive enhancement in He I took place between the region's two well-separated poles simultaneously with the development of an arch filament system seen in Hα.

Many examples in these data point to the occurrence of He I 'dark points' with the approach and sometimes merging of opposite polarity network. The enhancements show a wide variety of behavior from short-lived, flare-like darkenings to slow, but steady or variable increases in the He I λ10830 intensity. The ratio of dark points associated with 'chance' encounters of network and those associated with emerging bipoles has not yet been determined for this data set, but the approach and merging of flux appears to be a more common occurrence than the development of a ephemeral region. This has also been found in a study of the dynamics of the quiet sun magnetic fields by Martin *et al.* (1984). They find that two-thirds of the bipoles are explained by the converging motion of opposite polarity network and one-third results from the emergence of new flux.

5. He I Dark Points and Ephemeral Regions in Coronal Holes and High Speed Solar Wind Streams

Davis and Krieger (1980, 1982) found a correlation between the areal density of X-ray bright points observed in coronal holes and the density (and velocity) in the coronal hole-associated high speed streams in the solar wind. Recent theoretical work has also suggested that the emergence of small bipoles may play an important role in the acceleration of the solar wind in coronal holes (Akasofu, 1982; Pneuman, 1983). The He I 10830 and ephemeral region data used in this study provides the opportunity to test this correlation for a large sample of coronal holes observed during this cycle.

4.1. ASSOCIATION IN CORONAL HOLES

Coronal holes are easily identified in the 10830 He I spectroheliograms as brighter than quiet sun areas that show little or no network and have a predominately unipolar magnetic fields. A total of 61 coronal holes were selected from 1975 to 1984; 42 coronal holes had latitudes of $<25^\circ$ and 19 were $\geq 25^\circ$. Counts of He I 'dark points' and ephemeral regions were made during the three days of the central meridian passage of the 61 coronal holes. In Figure 9, the number of He I dark points per 10^{10} km^2 within the boundaries of the coronal holes has been plotted as a function of time. While there is a large variation in the areal density between individual coronal holes occurring for any given period, in general, the dark point counts in coronal holes vary anti-correlated with the solar cycle as is observed in the quiet sun. The curve shows a larger magnitude in change of the dark point numbers from sunspot minimum to maximum than is seen in the quiet sun dark point counts. Since dark points can be seen in coronal holes without the interference of chromospheric network, the larger variation in areal densities suggests that the identification of dark points in the quiet sun is influenced by the existence and

variability of He I network. A similar plot of the areal density of ephemeral regions in coronal holes shows a large scatter, but a variation in phase with the solar cycle comparable to the counts of ER over the entire sun during the same period.

The areal density of dark points and ephemeral regions has been compared with the absolute value of the average magnetic field strengths in 18 of the coronal holes measured by Harvey *et al.* (1982). The ephemeral region counts per 10^{10} km^2 show little (or perhaps a slight increase) with increasing coronal hole field strength. The number of dark points, however, decreases substantially at field strengths above 5G, then remains relatively level with increasing field strengths over 5G. All of the coronal holes with field strengths >5G occurred after mid-1978.

The locations of the He I dark points within coronal holes have been compared with the magnetic field data. All of the dark points in coronal holes were associated with bipolar structures. For coronal holes with latitudes $\leq 20^\circ$, 23% of the dark points were associated with ephemeral regions; 70% of the ephemeral regions corresponded to the locations of dark points. For coronal holes with latitudes $\leq 10^\circ$, the percentages change only slightly; 21% of the dark points were associated with ephemeral regions while 82% of the ER were associated with dark points. ~70% of the ephemeral regions were associated with He I 10830 dark points. A comparison with the statistics for the quiet sun averaged over the 1975-1984 period is shown in Table III.

Table III

Association of Dark Points (DP) and Ephemeral Regions (ER)

	% DP→ER	% ER→DP	%DP→bipole not ER
Coronal Hole	23	70	77
Quiet Sun	37%	40%	63%

This comparison suggests that the visibility of He I dark points associated with ephemeral regions is influenced by the λ10830 network, but that regardless of the surroundings two-thirds or more of the dark points are associated with bipolar structures interpreted as resulting from the chance encounter of existing opposite polarity network.

5.2. ASSOCIATION WITH HIGH SPEED SOLAR WIND STREAMS

The solar wind data published in the Interplanetary Medium Data Book (King, 1979, 1983) and in Solar Geophysical Data was used to identify the high speed solar wind streams associated with the 61 selected coronal holes. The high speed streams associated with coronal holes are recognized by an initial rapid increase then decrease in density (a compression front) followed by a slower increase in velocity and temperature. The onset of the stream was taken at the time of the density increase and its end when the velocity decreased to previous levels or reached a minimum. Solar wind data was available in these two sources through September 1982 for a several day period following the central meridian passage (CMP) of 34 of these 61 coronal holes. For 5 of the coronal holes, no high speed stream could be detected in the 6 days after the the hole's central meridian passage. The peak and average (over the stream) values of bulk velocity (V_p, V_a), density (ρ_p, ρ_a), and temperature (T_p, T_a) of the high speed streams were compared with the areal density of dark points and ephemeral regions determined for the 29 associated coronal holes. The results are shown in Figures 11, 12 and 13.

For each of the comparisons, a straight line of the form Y = A +bx has been fitted to the data using the bevington least squares routine; Y is the solar wind parameter, A and b are constants determined by a fit to the data, and x the areal density of dark points (DP) or ephemeral regions (ER) within the boundaries of the associated coronal hole. Shown in Table IV are the determined correlation coefficient (r) compared with r_{abs}, the absolute value of a correlation coefficient for n-2 degrees of freedom and 2 variables (taken from Table 7, Statistics Manual by E. Crow, F. A. Davis, and Maxfield, M.W., 1960, p. 241). If $|r| > r_{abs}$, the two considered parameters are correlated at a 95% confidence level.

Table IV

Dark Point (DP) and Ephemeral Region (ER) Correlation with High Speed Solar Wind Stream Parameters

	Coronal Holes all Latitudes				Coronal Holes of Latitudes <25			
	r		r_{abs}	Correlated	r		r_{abs}	Correlated
$V_a \rightarrow DP$	0.356	<	0.367	no	0.437	~	0.433	?
$V_a^p \rightarrow DP$	0.428	>	0.367	yes	0.600	>	0.433	yes
$\rho_p \rightarrow DP$	0.390	>	0.381	?	0.362	<	0.456	no
$\rho_a \rightarrow DP$	0.312	<	0.374	no	0.205	<	0.444	no
$T_a \rightarrow DP$	0.373	~	0.374	?	0.529	>	0.444	yes
$T_a^p \rightarrow DP$	0.465	>	0.374	yes	0.546	>	0.444	yes
$V_a \rightarrow ER$	-0.060	<	0.367	no	-0.129	<	0.433	no
$V_a^p \rightarrow ER$	-0.110	<	0.367	no	-0.372	<	0.433	no
$\rho_p \rightarrow ER$	0.165	<	0.381	no	0.310	<	0.456	no
$\rho_a \rightarrow ER$	0.152	<	0.374	no	0.398	<	0.444	no
$T_a \rightarrow ER$	0.151	<	0.374	no	0.256	<	0.444	no
$T_a^p \rightarrow ER$	0.117	<	0.374	no	0.106	<	0.444	no

The equation for a least squares fit between the high speed stream parameters that are correlated with the areal density of dark points are shown below along with the σ's for the constants A and b:

For coronal holes at all latitudes,

Average velocity (km s^{-1}):	V_a =455.8+ 16.3xDP	σ_A =±20.0	σ_b =± 6.6
Average temperature (x10^3 K):	T_a^p= 94.0 + 12.0xDP	σ_A =±13.3	σ_b =± 1.5

For coronal holes with latitudes ≤25°.

Average velocity (km s^{-1}):	V_a =438.1 + 24.3xDP	σ_A =±21.7	σ_b =± 7.5
Peak temperature (x10^3 K):	T_a =228.5 + 31.9xDP	σ_A =±16.3	σ_b =±16.3
Average temperature (x10^3 K):	T_a^p= 92.9 + 15.9xDP	σ_A =±16.3	σ_b =± 5.7

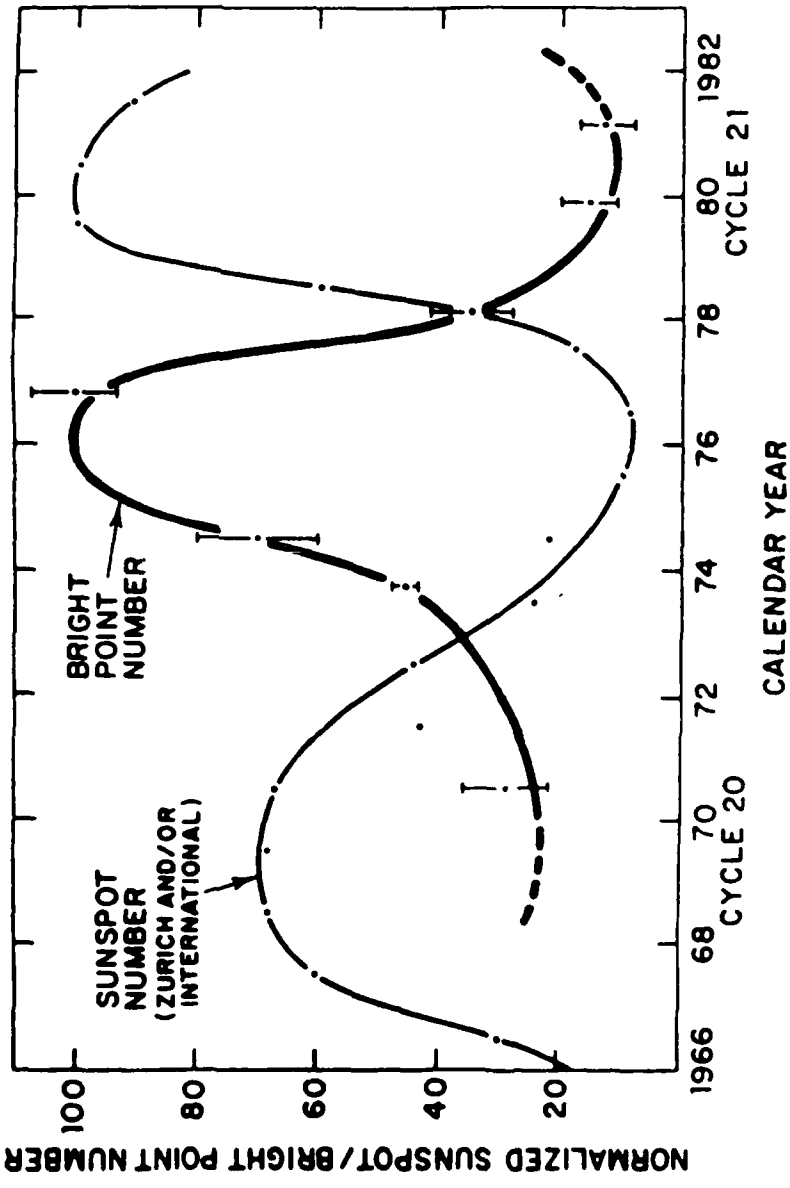
NORMALIZED SUNSPOT/BRIGHT POINT NUMBER
100
80
60
40
20
1966
68
70
72
74
76
78
80
1982
CYCLE 20
CYCLE 21
CALENDAR YEAR
BRIGHT POINT NUMBER
SUNSPOT NUMBER (ZURICH AND/OR INTERNATIONAL)

Figure 6

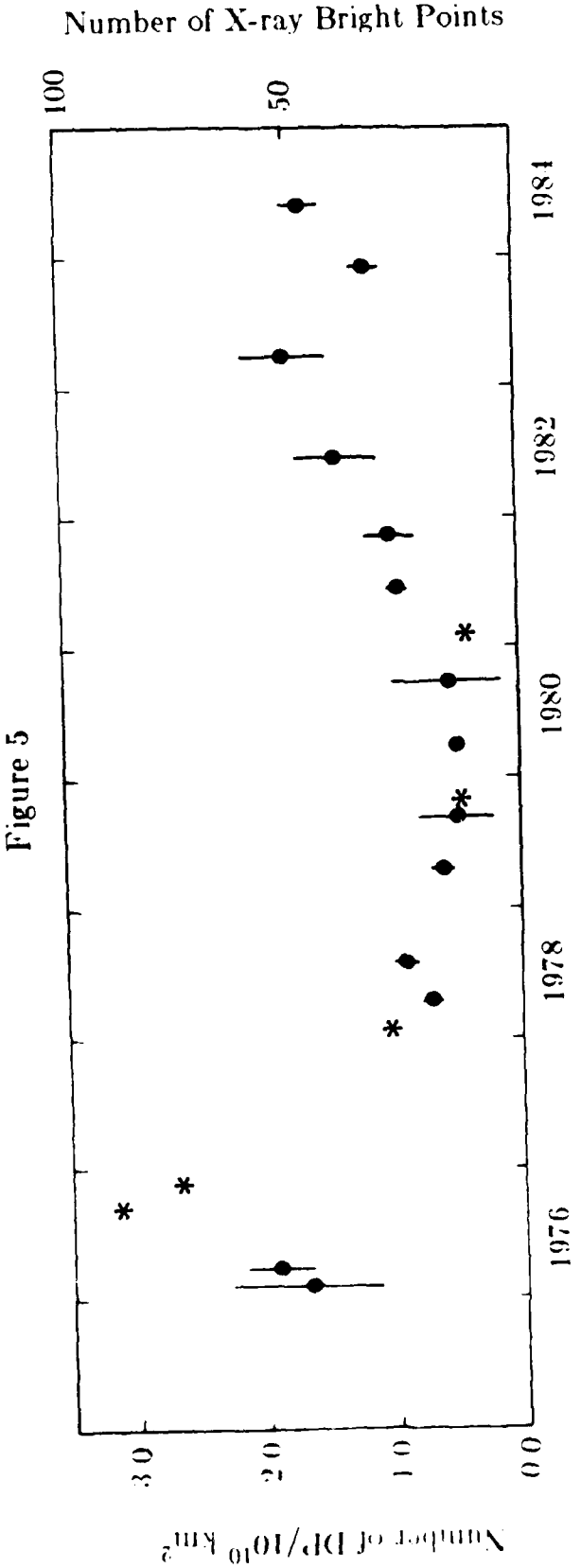
Number of X-ray Bright Points
100
50
1984
1982
1980
1978
1976
30
20
10
00
Number of DP/10^10 km^2

Figure 5

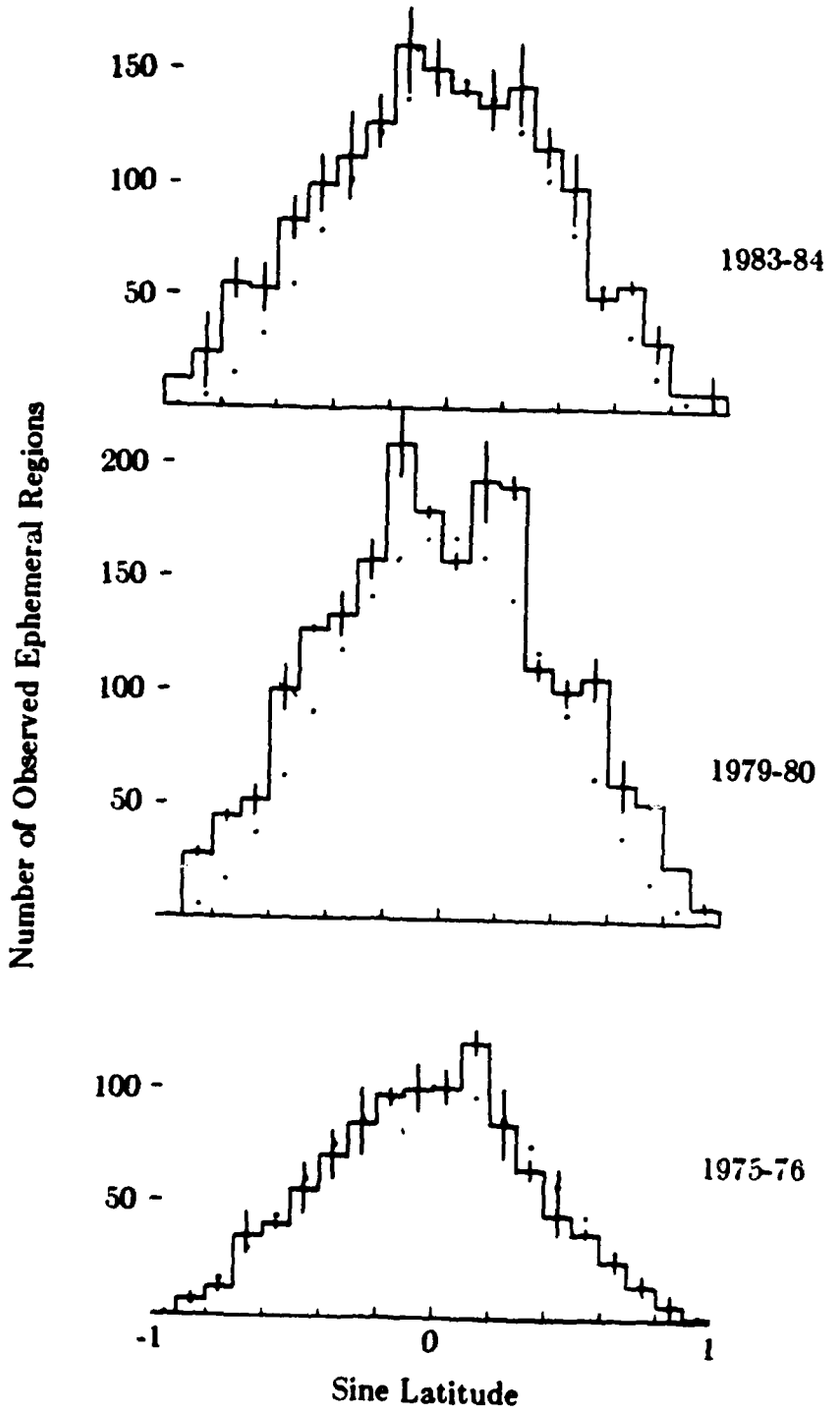
150
100
50
1983-84
200
150
100
50
1979-80
100
50
1975-76
Number of Observed Ephemeral Regions
-1
0
1
Sine Latitude

Figure 4

Figure 3

(From Tang *et al.*, Solar Phys. 91, 75)

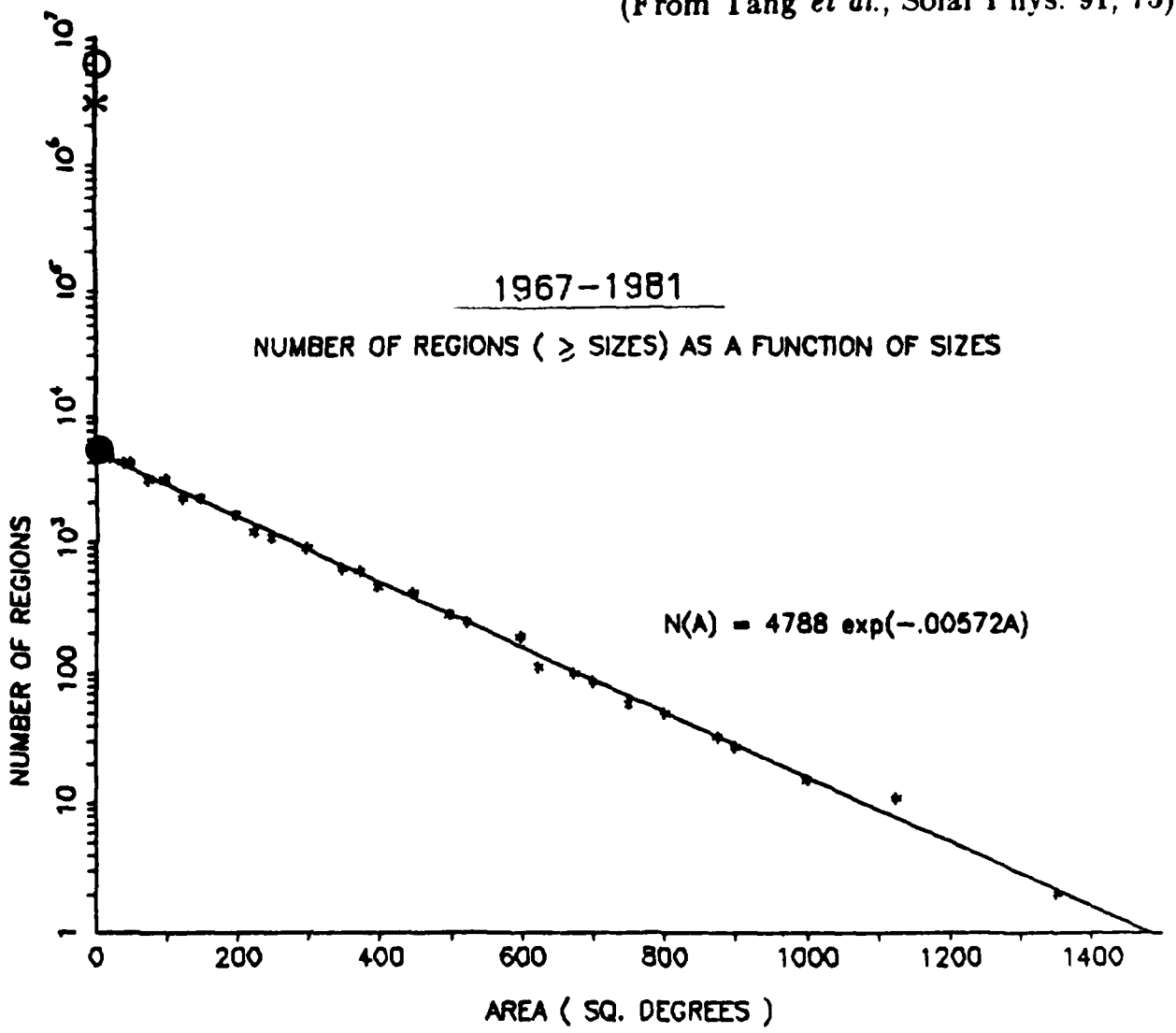

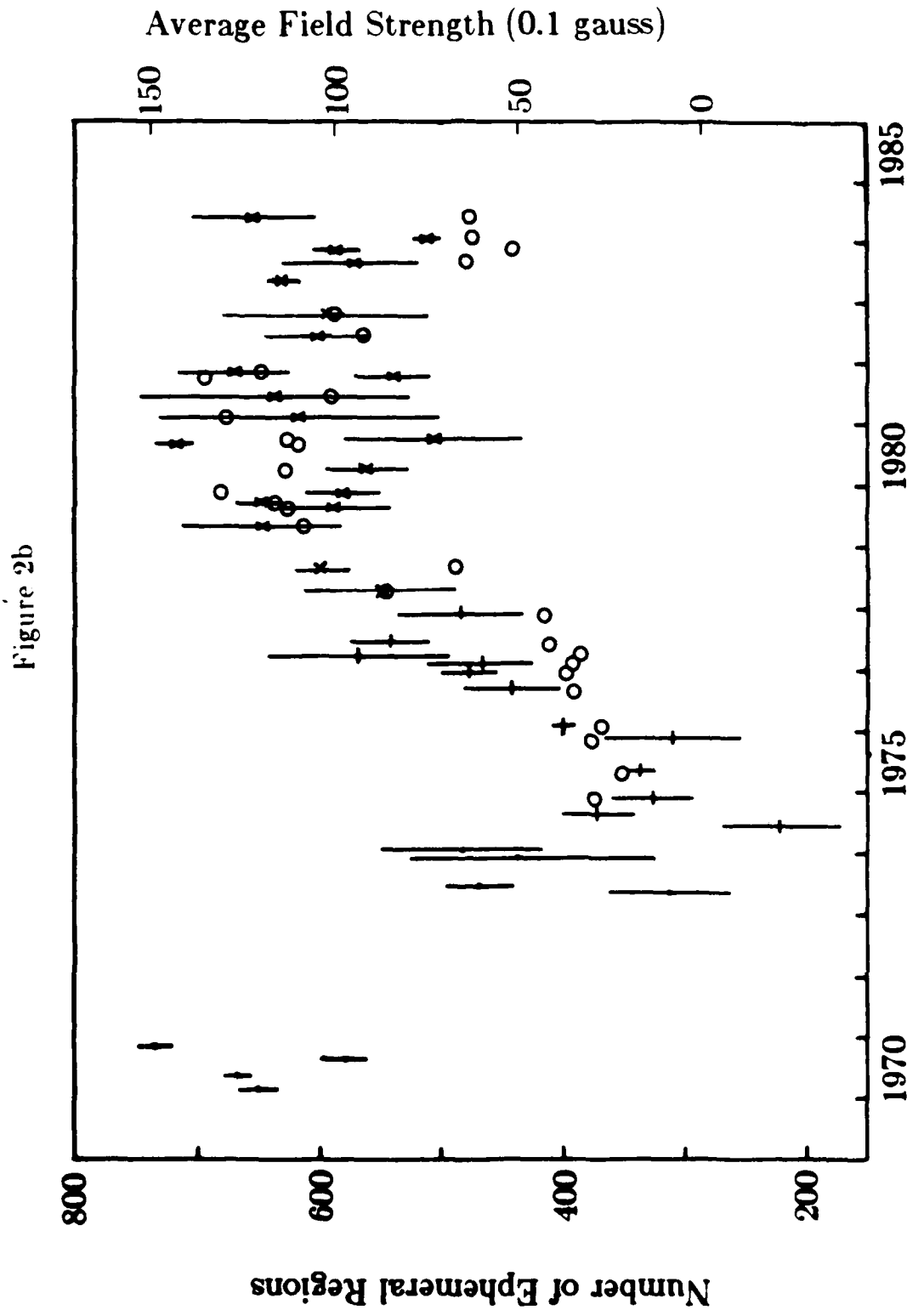
Average Field Strength (0.1 gauss)
150
100
50
0
1985
1980
1975
1970
800
600
400
200
Number of Ephemeral Regions

Figure 2b

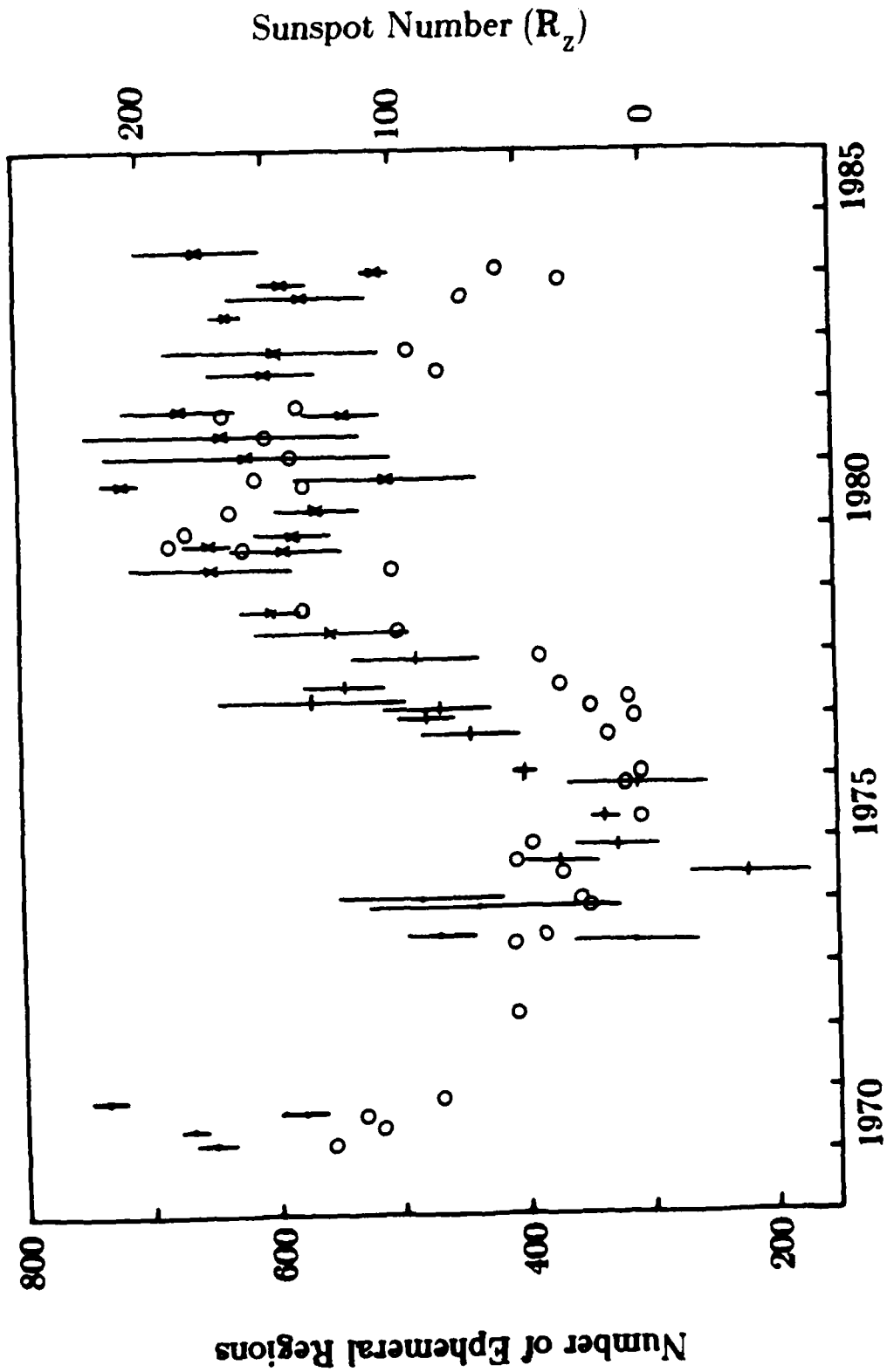
Sunspot Number (R_z)
200
100
0
1985
1980
1975
1970
800
600
400
200
Number of Ephemeral Regions

Figure 2a

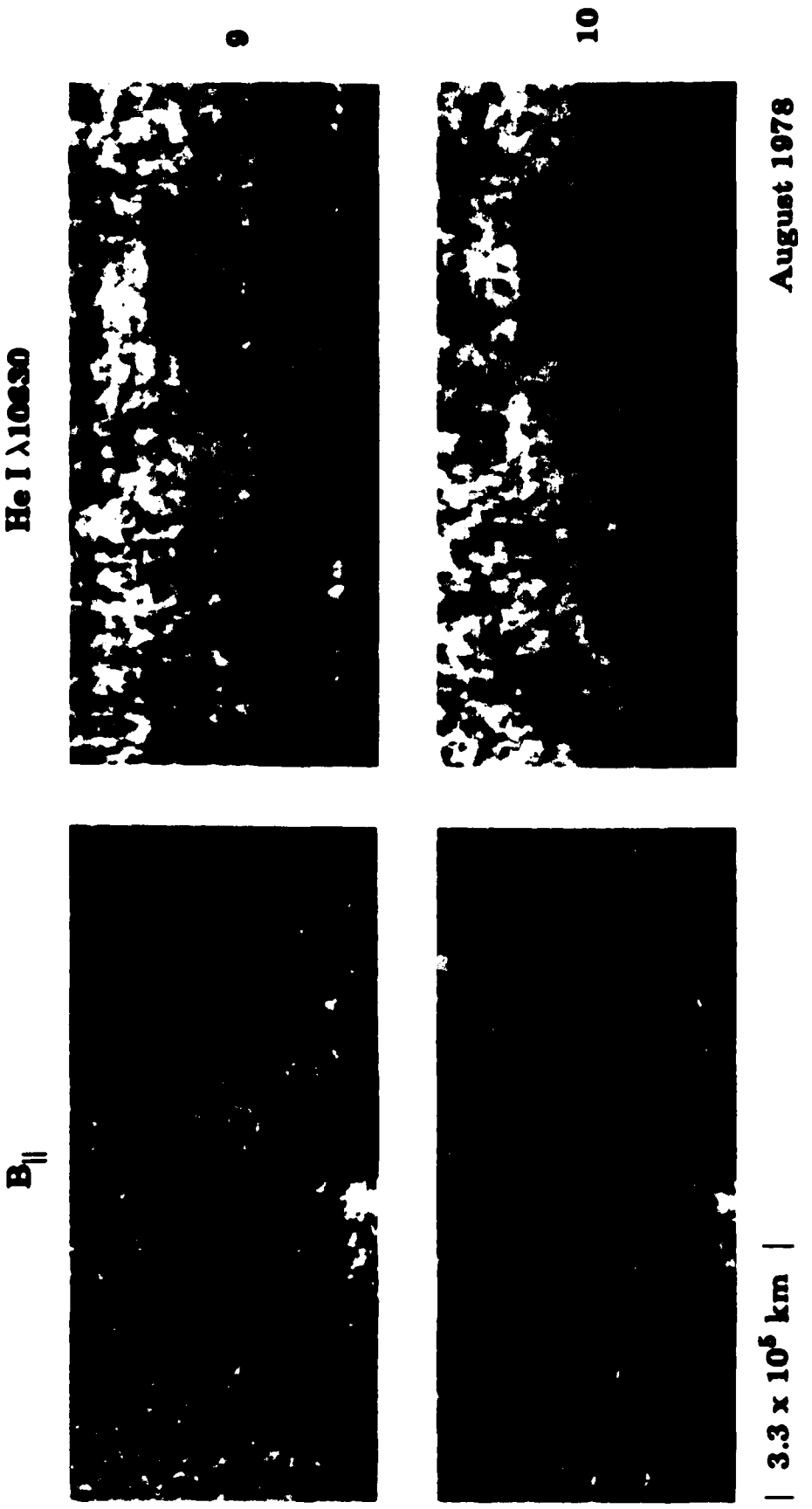

Figure 1

filament system (Hα) and a darkening in He I λ10830 late in this observational sequence. In the lower portion of the pictures, two opposite polarity network elements approach each other and merge. A loop connecting them can been seen in Hα at 2013 UT along with a He I 'dark point', which fluctuates substantially in intensity.

Fig. 9 - Areal density of He I λ10830 'dark points' within the boundaries of coronal holes as a function of time. To avoid confusion in this graph, no error bars are shown.

Fig. 10 - Areal density of ephemeral regions (bottom) and He I λ10830 'dark points' (top) within the boundaries of coronal holes as a function of the coronal hole's average magnetic field strength. Vertical lines indicate estimated errors.

Fig. 11 - Area density within coronal holes of ephemeral regions (left) and He I dark points (right) as a function of the average (bottom) and peak (top) bulk velocity of the associated high-speed solar wind stream. Data from 1975-77 and 1982 is indicated by ● and from 1978-1981 by ✱.

Figure 12 - Area density within coronal holes of ephemeral regions (12a) and He I dark points (12b) as a function of the average (bottom) and peak (top) density of the associated high-speed solar wind stream. Data from 1975-77 and 1982 is indicated by ● and from 1978-1981 by ✱.

Figure 13 - Area density within coronal holes of ephemeral regions (13a) and He I dark points (13b) as a function of the average (bottom) and peak (top) temperature of the associated high-speed solar wind stream. Data from 1975-77 and 1982 is indicated by ● and from 1978-1981 by ✱.

Figure 14 - Plot of the area of mixed polarity on the Sun between $\pm 60^\circ$ latitude compared with the sunspot number (from Giovanelli, *Solar Phys* **77**, 27).

Figure 15 - Plot of the area of mixed polarity on the Sun between $\pm 60^\circ$ latitude (from Giovanelli, *Solar Phys* **77**, 27), compared with the number of X-ray bright points (from Davis, *Solar Phys* **88**, 337).

Figure Captions

Fig. 1 Sections of the full disk photospheric magnetograms and He I λ10830 spectrheliograms from two successive days, 9 and 10 August 1978, showing the identifications of newly emerged flux (□) and of encounters of existing opposite polarity network (▶ ◀).

Fig. 2 Number of ER on the Sun at any given time from 1970 through mid-1984. Estimated errors are indicated by vertical lines. 40-channel data (•); 512-channel data, high gain (+) and low gain (x). The number of ER are compared in Figure 2a with the sunspot number (○) for the same time periods as considered for the ER and in Figure 2b with the total magnetic flux (○) on the Sun. The sunspot data is from Solar Geophysical Data and the total flux ($|\Phi_+| + |\Phi_-|$) has been determined from the synoptic magnetic field observations constructed for each Carrington rotation of the Sun from the daily magnetic field observations. No correction has been made for saturation in sunspots or for foreshortening toward the poles.

Fig. 3 - The number of active regions of a given size and greater as a function of size (from Tang *et al.*, *Solar Phys.* 91, 75). If ephemeral regions are small active regions, the circle (•) indicates the expected number of ER and all active regions of greater size. Subtracting off the active regions yields $2x10^3$ ER. The circle (○) is the number of ER estimated from Figure 2 assuming an average ER lifetime of 12 hours and the * is the number of ER assuming an average ER lifetime of 18 hours.

Fig. 4 - The latitude distribution of observed ephemeral regions during three phases of the current solar cycle. Vertical lines indicate estimated errors. A uniform distribution curve (•) has been determined by application of the visibility function to the average number of ER observed between +.1 and -.1 in sine latitude.

Fig. 5 Areal density of He I λ10830 'dark points' (●) in quiet sun areas within a radius vector of 0.4 as a function of time and compared with counts of X-ray bright points (*).

Fig. 6 Variation of X-ray bright points from 1970 to 1981 compared with sunspot numbers (from Davis, J.M.: 1983, *Solar Phys.* **88**, 337).

Fig. 7 Comparison of a soft X-ray image of an area of the sun and the corresponding photospheric magnetic fields (from Golub *et al.*, 1977, Figure 1, p. 114). The re-analysis of the identification of ephemeral regions has been made using the full disk magnetograms from 20 and 21 August 1973. Ephemeral regions that emerged since 20 August are indicated by a circle; 'chance' encounters of opposite polarity network flux are indicated by an adjacent arrow.

Fig. 8 A time sequence of Hα filtergrams, the photospheric magnetic fields and He I λ10830 spectroheliograms of an area of quiet sun. The concentric alternating pattern of black and white in the magnetic field observations indicate saturation in the data; the polarity is defined by the outermost color. An ephemeral region can be seen emerging in the upper portion of pictures and is associated with an arch

Livingston, W., Harvey, J., and Slaughter, C.: 1971, *Proc. 11th Coll. of the IAU*, Edinburgh August 1970, 52.

Livingston, W.C., Harvey, J.W., Slaughter, C.D., and Trumbo, D.: 1976, *Appl. Opt.* **15**, 40.

Martin, S.F. and Harvey, K.L.: 1979, *Solar Phys.* **64**, 93.

Martin, S.F., Livi, S.H.B, Wang, J., and Shi, Z.: 1984, Proceedings of the Workshop on Measurements of Solar Vector Magnetic Fields, Marshall Space Flight Center, 15-18 May 1984, in press.

Piddington, J.H.: 1978a, *Astrophys. and Space Sci.* **55**, 401.

Piddington, J.H.: 1978b, preprint.

Pneuman, G.W.: 1983, *Astrophys. J.* **265**, 468.

Sheeley, N.R., Jr. and Harvey, J.: 1981, *Solar Phys.* **70**, 237.

Tang, F., Howard, R., and Adkins, J.M.: 1984, *Solar Phys.* **91**, 75.

high speed stream parameters during the period of cycle minimum may be a consequence of the more stable and longer-lived coronal holes that are present at that time compared to the less stable and more active conditions as the cycle develops.

While this result is statistical, it may be that by following individual coronal holes and the associated high speed solar wind streams over their lifetime could yield a better correlation between dark point counts (and ephemeral regions) and high speed stream parameters (as was reported by Davis and Krieger (1980, 1982) for the coronal holes observed during 1973). This has not done as part of this analysis, but will be followed up at a later date.

7. Acknowledgements

A special thank you to J. Harvey, N. R. Sheeley, C. Zwaan for their many and useful discussions and helpful assistance.

8. References

Akasofu, S.: 1982, Abstracts, 24th COSPAR meeting held May 16-June in Ottawa, Canada, p. 10.

Davis, J.M.: 1983, *Solar Phys.* **88**, 337.

Davis, J.M.: 1984, *Solar Phys.*, in press.

Davis, J.M., Golub, L., and Krieger, A.S.: 1977, *Astrophys. J.* **214**, L141.

Davis, J.M. and Krieger, A.S.: 1980, *Bull. Amer. Astron. Soc.* **12**, 518.

Davis, J.M. and Krieger, A.S.: 1982, Abstracts, 24th COSPAR meeting held May 16-June in Ottawa, Canada, p. 25.

Giovanelli, R.G.: 1982, *Solar Phys.* **77**, 27.

Golub, L.: 1980, *Phil Trans R Soc London* **A297**, 595.

Golub, L., Davis, J.M., and Krieger, A.S.: 1979, *Astrophy. J.* **229**, L145.

Golub, L., Krieger, A.S., Harvey, J.W., and Vaiana, G.: 1977, *Solar Phys* **53**, 111.

Golub, L. Krieger, A.S., Silk, J.K., Timothy, A.F., and Vaiana, G.S.: 1974, *Astrophy. J.* **189**, L93.

Harvey, K.L., Harvey, J.W., and Martin S.F.: 1975, *Solar Phys* **40**, 87.

Harvey, K.L. and Harvey, J.W.:1976, Air Force Geophysics Laboratory Report AFGL-TR-76-0255, Part II. ADA038124

Harvey, J.W., Krieger, A.S., Timothy, A.F., and Vaiana, G.S.: 1975, *Observazioni e Memorie Osservatorio de Arcetri*, **104**, 50.

Harvey, K.L., Sheeley, N.R., Jr., and Harvey, J.W.: 1982, *Solar Phys.* **79**, 149.

King, J.H.: 1979, Interplanetary Medium Data Book - Supplement 1, NSSDC/WDC-A-R&S 79-08.

King, J.H.: 1983, Interplanetary Medium Data Book - Supplement 2, NSSDC/WDC-A-R&S 83-01.

magnetic bipoles resulting from the encounters of existing flux can only be done reliability with time sequence data. The probability of a 'chance' encounter taking place between network of opposite polarity, however, depends on the degree of mixing between the positive and negative fields, i.e., the area of mixed polarity on the Sun. Giovanelli (1982) has measured the fractional area of mixed polarities on the Sun between the latitudes $\pm 60^\circ$ from 1972 to 1981. His results are shown in Figure 14 in comparison with the sunspot numbers. As can be seen from this graph, the area of mixed polarity varies inversely with the solar cycle. When the number of X-ray Bright Points are added to this plot (Figure 15), we find a good correlation between the variation of XBP and the area of mixed polarity. This suggests that the anti-correlation of He I dark points' and XBP with the sunspot cycle may indeed be explained by a close association with 'chance' encounters of existing network of opposity polarities.

3. An association was found between the areal density of He I dark points in coronal holes with the solar cycle and with the average magnetic field strength of the coronal holes. Harvey *et al.* (1982) has suggested that the increase of the magnetic field strengths in coronal holes after mid-1978 is due to the general increase in magnetic flux levels on the Sun with the increased emergence of active regions (AR) during the rise of the solar cycle. With the increased production of active regions, particularly in AR complexes, coronal holes are more subject to change in size, shape, position and magnetic flux densities (supplied by the remnants of old active regions). During minimum, with the activity level much reduced, coronal holes evolve more slowly. Davis (1984) has found that the X-ray bright point counts per unit area in three low latitude coronal holes observed during 1973 increased as the coronal hole aged. At the coronal holes' formation, the XBP areal densities within the their boundaries were also at about the same level as in the nearby quiet sun.

These two studies suggest that the correlation of the dark point areal densities in coronal holes with the magnetic field strength of the coronal hole (and therefore with the solar cycle) may be explained by the evolution and history of the coronal holes. For example, during high levels of activity in the solar cycle, coronal holes are changing significantly from one rotation to the next due to the influences of nearby active regions, rather than by the decay as the magnetic fields disperse by random motions and differential rotation. The dark point (and XBP) counts, therefore, may be lower such as in the newly formed coronal holes discussed by Davis (1984). At minimum or extended periods of low activity, the coronal holes decay 'normally', their field strengths decreased, the production of dark points and X-ray bright points increases. Such an explanation suggests that the increase of dark point counts in 1982 (Figure 5) would correspond to an overall decrease in the coronal hole field strengths.

4. A correlation is suggested between the areal densities of dark points and of ephemeral regions in coronal holes (determined during their central meridian passage) and some of the parameters of the associated high speed streams in the solar wind. This relation appears to vary with the solar cycle. For example, over the solar cycle , the average velocity and the peak and average temperature observed in the high speed stream appears related to the counts of dark points; no similar correlation was found with ephemeral region counts. But in comparisons of the data between the periods of solar minimum and lower activity (1975-1977, 1982) to the more active periods (1978-1981), higher correlation coefficients are found during the minimum activity years than for sunspot maximum years. This is particularly true for the ephemeral region counts which appear to be fairly well correlated with the velocity, density and temperature of the high speed streams. The better association between ephemeral regions and dark points with

Cycle Minimum Years (1975-77, 1982)

Temperature ($x10^3$ °K):	$T = 78.4 + 59.8xDP$	$\sigma_A = \pm 76.6$	$\sigma_b = \pm 20.9$
	$T_p = 73.2 + 17.8xDP$	$\sigma_A = \pm 29.0$	$\sigma_b = \pm 7.9$
Velocity (km s^{-1}):	$V = 425.0 + 175.0xER$	$\sigma_A = \pm 55.3$	$\sigma_b = \pm 49.1$
	$V_p = 450.6 + 76.2xER$	$\sigma_A = \pm 31.1$	$\sigma_b = \pm 27.6$
Density (cc^{-1}):	$\rho_p = -5.4 + 31.9xER$	$\sigma_A = \pm 13.1$	$\sigma_b = \pm 11.4$
Temperature ($x10^3$ °K):	$T = 91.5 + 181.7xER$	$\sigma_A = \pm 65.0$	$\sigma_b = \pm 56.5$
	$T_s = 73.2 + 57.7xER$	$\sigma_A = \pm 24.0$	$\sigma_b = \pm 20.9$

Cycle Maximum Years (1978-1981)

Density (cc^{-1}):	$\rho_p = 6.7 + 7.6xER$	$\sigma_A = \pm 5.4$	$\sigma_b = \pm 3.2$
	$\rho_p = 4.4 + 2.3xER$	$\sigma_A = \pm 1.8$	$\sigma_b = \pm 1.1$

This analysis suggests that there is a relation between the areal density of dark points and ephemeral regions and some of the selected parameters of solar wind streams. A better correlation between these parameters is found during the period of solar cycle minimum than during maximum. For entire data set from 1975-1984, the dark point counts measured during a coronal hole's central meridian passage are a slightly more significant parameter than ephemeral regions; during cycle minimum, however, the counts of ephemeral regions in coronal holes tend to be better correlated with the high speed solar wind stream parameters than dark points.

6. Conclusions

This study of ephemeral regions and their association with He I λ10830 dark points suggests the following conclusions:

1. The occurrence of ER varies nearly in phase with the solar cycle with the minimum preceding sunspot minimum by at least one year and coinciding with the minimum in the Sun's total observed magnetic flux. The increase by only a factor of two from minimum to maximum in the number of ER and the total number of ER ($3\text{-}4.5x10^6$) estimated to emerge during a solar cycle indicates that these small-scale regions are not small active regions. It does support the idea that ephemeral regions are primarily a surface phenomenon perhaps resulting from convective twisting of sub-photospheric quiet sun magnetic fields as has been suggested by Piddington (1978a, 1978b). In such a case, the variation of the numbers of ER over the solar cycle are closely related to the changes in the total magnetic flux on the Sun from the dispersed fields of old active regions as the solar cycle develops and to the spatial pattern of those fields.

2. Almost 90% of the dark points observed in He I λ10830 were associated with small bipoles. It has also been found that the number of dark points varies anti-correlated to the solar cycle. The high association with magnetic bipoles and the observed variation during the solar cycle supports the premise that He I dark points correspond to X-ray bright points. The observations suggest that He I 'dark points' and, therefore, XBP occur with the emergence of some ER, but more often with the encounter of existing network flux of opposite polarities. This is true both in the quiet sun, though there is some question that some dark points are not being detected, and in coronal holes, where there is little confusion with the chromospheric network and structures. The determination of

The correlation between velocity and the dark point counts appears to confirm the results of Davis and Krieger (1980, 1982), but their finding of and association between density in high speed streams and the areal density of X-ray bright points is not substantiated with the dark point data. No correlation was found between ephemeral region counts in coronal holes and the high speed stream parameters.

Because the nature of coronal holes changes from the sunspot minimum to sunspot maximum years, the coronal hole data and associated high speed stream data was divided into two subsets: (1) 1975-1977 and 1982, and (2) 1978-1981. The correlation between the high speed solar wind stream parameters and the associated coronal hole dark point and ephemeral region areal densities is shown in Table V between these two periods.

Table V

Dark Point (DP) and Ephemeral Region (ER) Correlation
with High Speed Solar Wind Stream Parameters
for the Sunspot Minimum and Sunspot Maximum Years

	Coronal Holes 1975-1977, 1982				Coronal Holes 1978-1981			
	r		r_{abs}	Correlated	r		r_{abs}	Correlated
$V_p \rightarrow DP$	0.427	$<$	0.514	no	-0.042	$<$	0.497	no
$V_a^p \rightarrow DP$	0.512	$\sim$	0.514	?	0.029	$<$	0.497	no
$\rho_p \rightarrow DP$	0.360	$<$	0.532	no	-0.060	$<$	0.514	no
$\rho_a^p \rightarrow DP$	0.531	$\sim$	0.532	?	-0.025	$<$	0.514	no
$T_p \rightarrow DP$	0.671	$>$	0.532	yes	-0.031	$<$	0.514	no
$T_a^p \rightarrow DP$	0.580	$>$	0.533	yes	0.300	$<$	0.514	no
$V_p \rightarrow ER$	0.732	$>$	0.514	yes	-0.404	$<$	0.497	no
$V_a^p \rightarrow ER$	0.640	$>$	0.514	yes	-0.469	$<$	0.497	no
$\rho_p \rightarrow ER$	0.664	$>$	0.532	yes	0.563	$>$	0.514	yes
$\rho_a^p \rightarrow ER$	0.521	$<$	0.532	no	0.534	$>$	0.514	yes
$T_p \rightarrow ER$	0.713	$>$	0.532	yes	0.268	$<$	0.514	no
$T_a^p \rightarrow ER$	0.658	$>$	0.532	yes	0.150	$<$	0.514	no

Based on this table, there appears to be a difference in the association of high speed stream parameters and the areal density of dark points and ephemeral regions in coronal holes between the low and high activity years. For almost all of the comparisons, the correlation coefficients are higher between the considered parameters during the cycle minimum years, when the coronal holes are longer lived and more stable, than the coefficients during the higher sunspot activity years. The correlation between the average velocity in high speed streams and the dark points counts seen for the entire data set is now marginal in this division of the data; a marginal correlation is now found between the dark points and the average density in high speed streams. The equations between the correlated parameters are listed below:

21 AUGUST 1973

1622UT AS&E

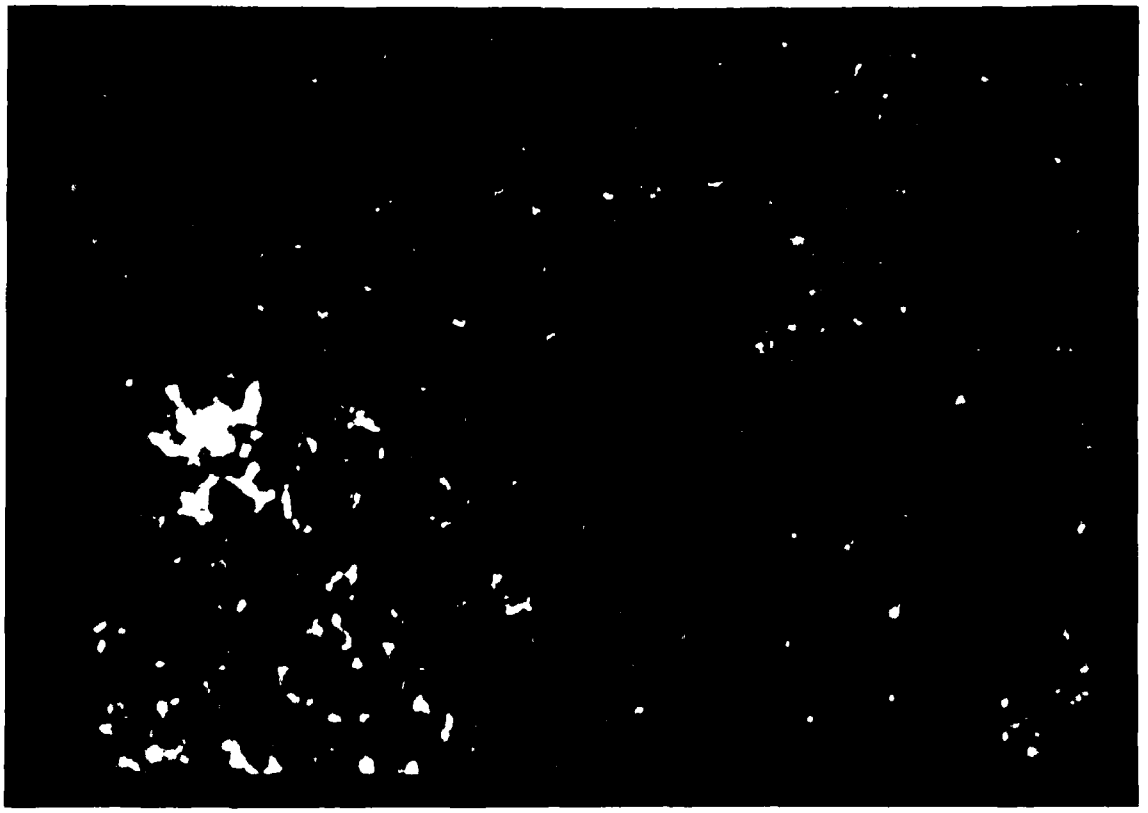

1520-1620UT KPNO

Figure 7

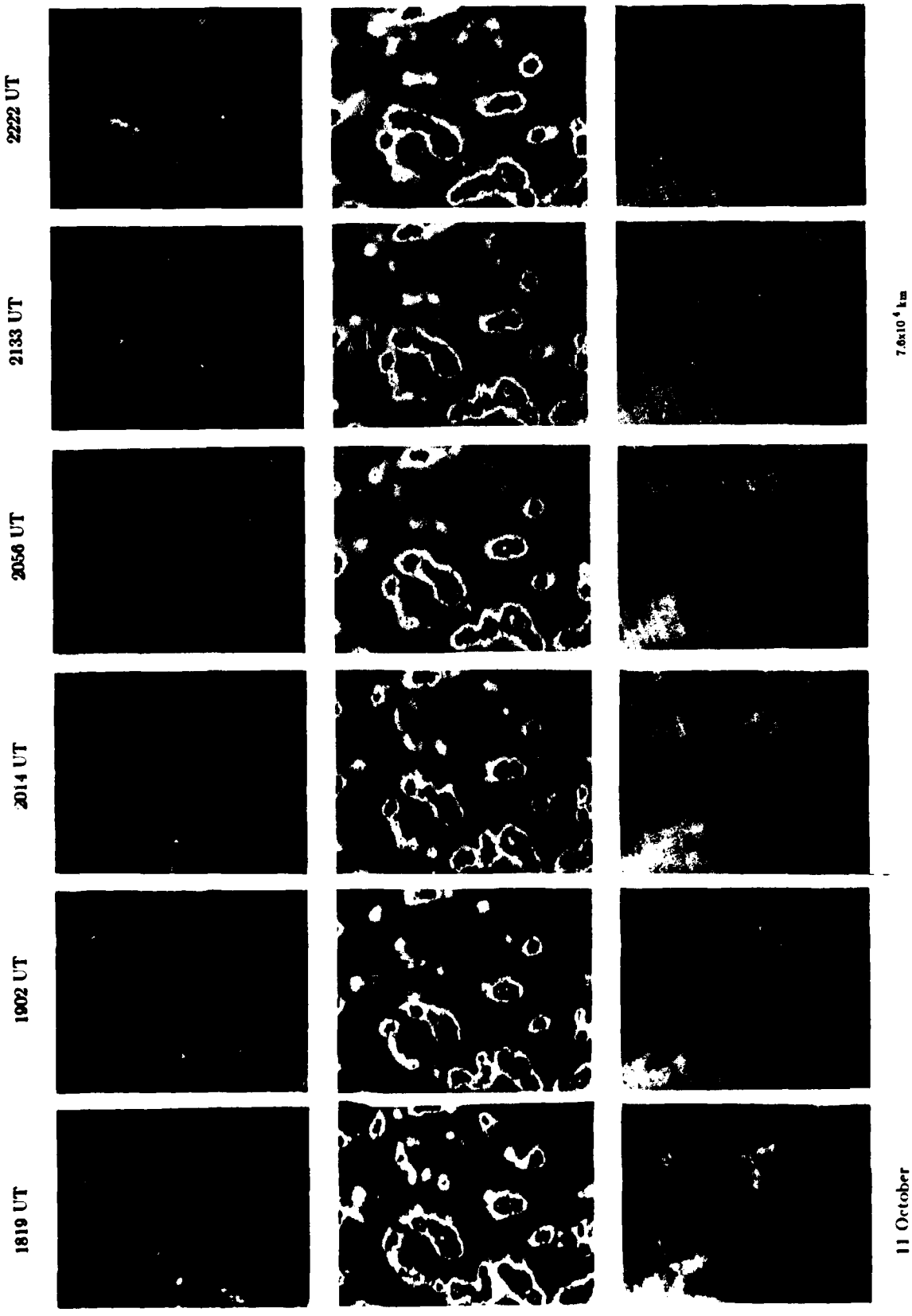
1819 UT
1902 UT
2014 UT
2056 UT
2133 UT
2222 UT
11 October
7.6x10⁴km

Figure 8

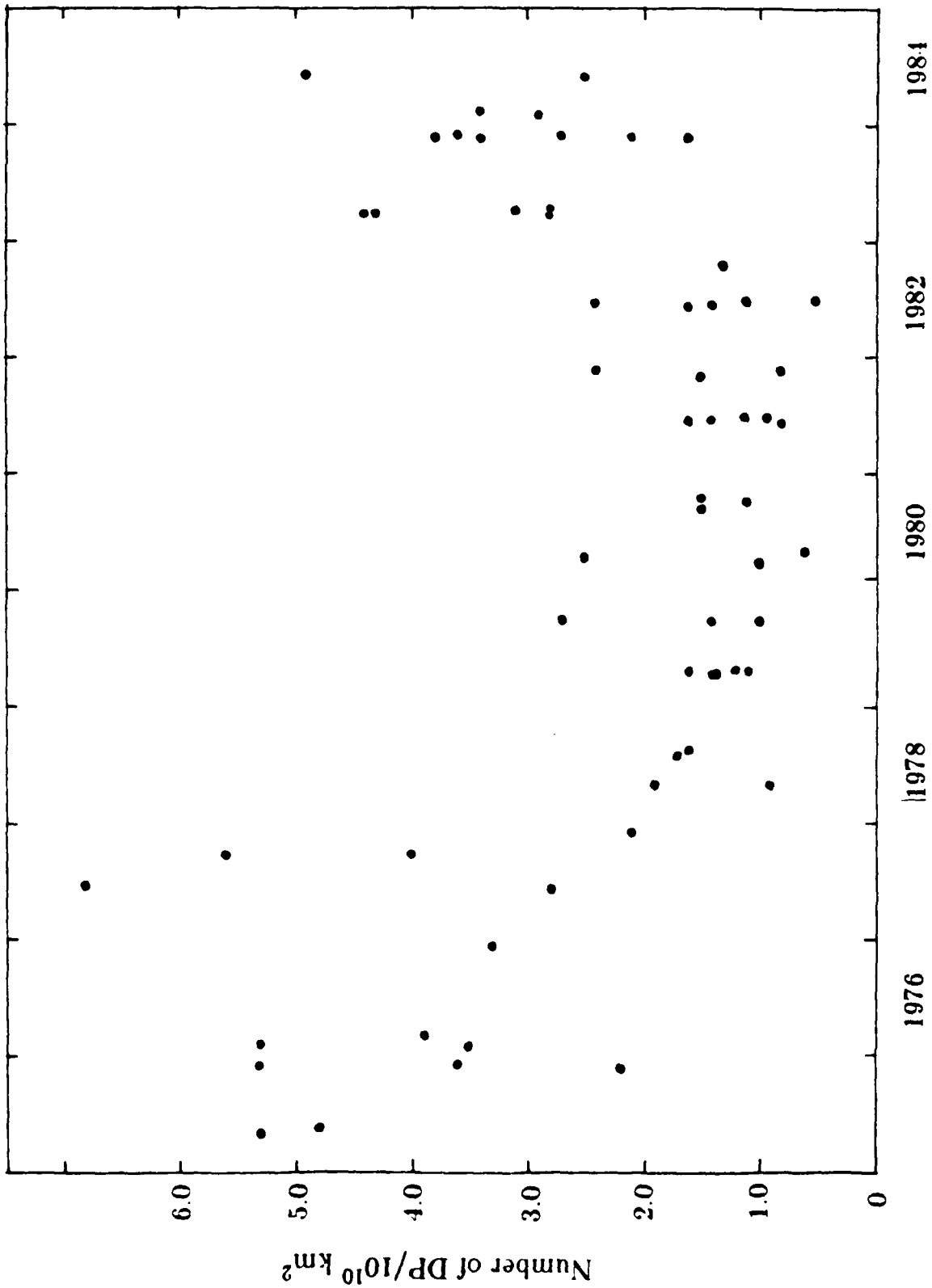
Number of DP/10^{10} km^2
0
1.0
2.0
3.0
4.0
5.0
6.0
1976
1978
1980
1982
1984
Year

Figure 9

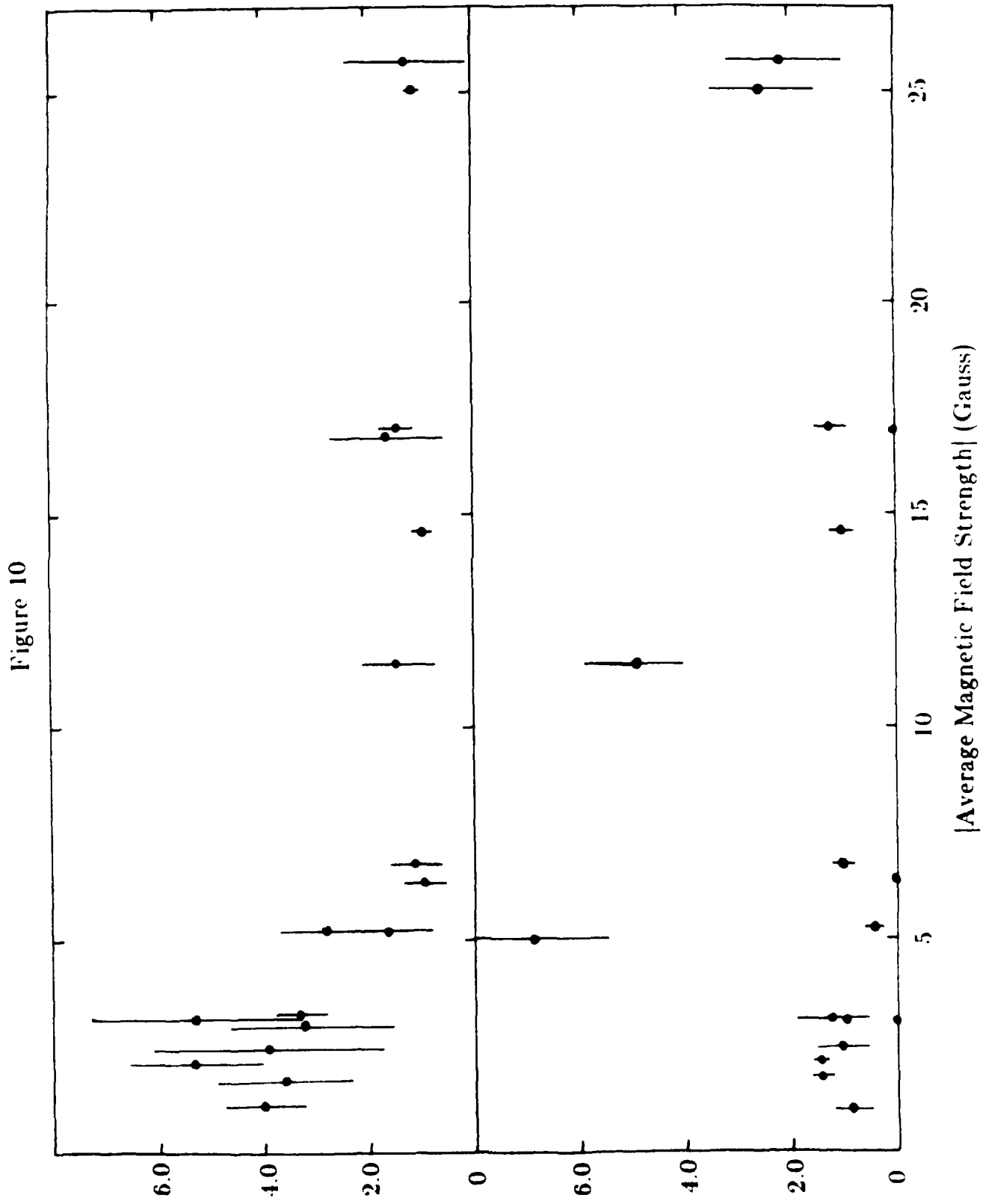
Number of DP/10^10 km^2
Number of ER/10^10 km^2
0
2.0
4.0
6.0
5
10
15
20
25
|Average Magnetic Field Strength| (Gauss)

Figure 10

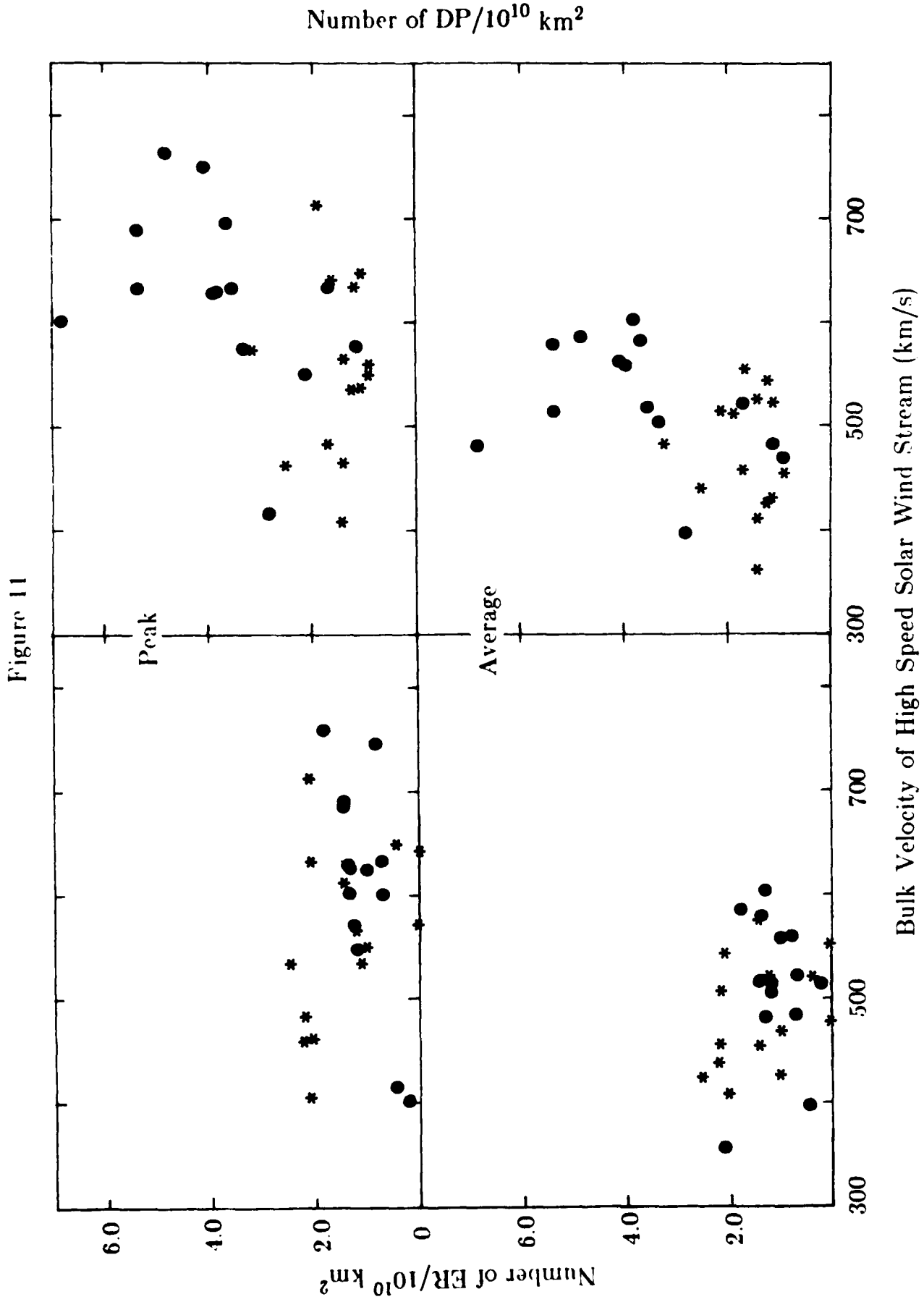
Number of DP/10^10 km^2
Peak
Average
Number of ER/10^10 km^2
0
2.0
4.0
6.0
300
500
700
Bulk Velocity of High Speed Solar Wind Stream (km/s)

Figure 11

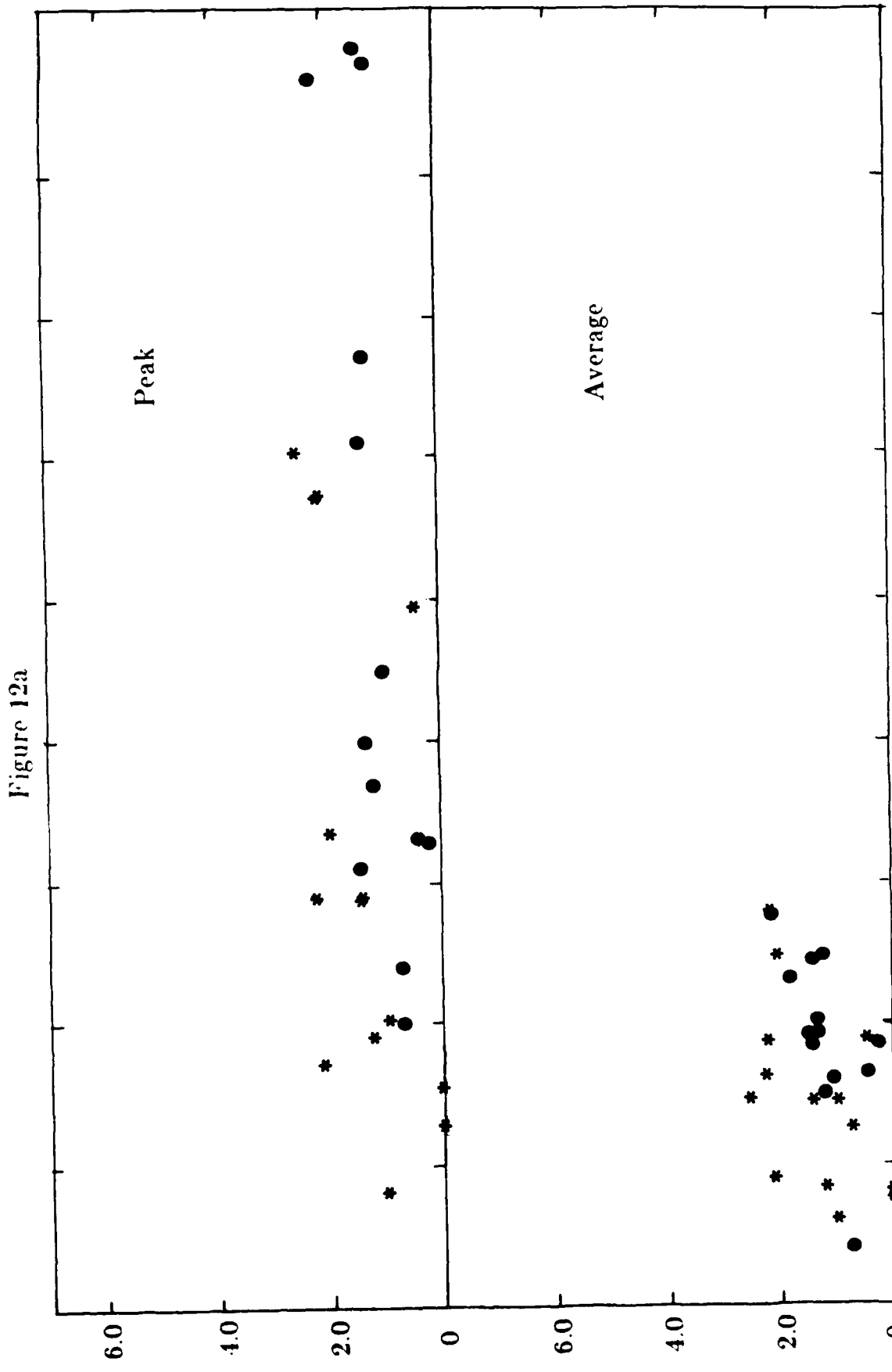
Peak
Average
6.0
4.0
2.0
0
5
10
15
20
25
30
35
40
Number of ER/10^10 km^2
Ion Density of High Speed Solar Wind Streams (per cc)

Figure 12a

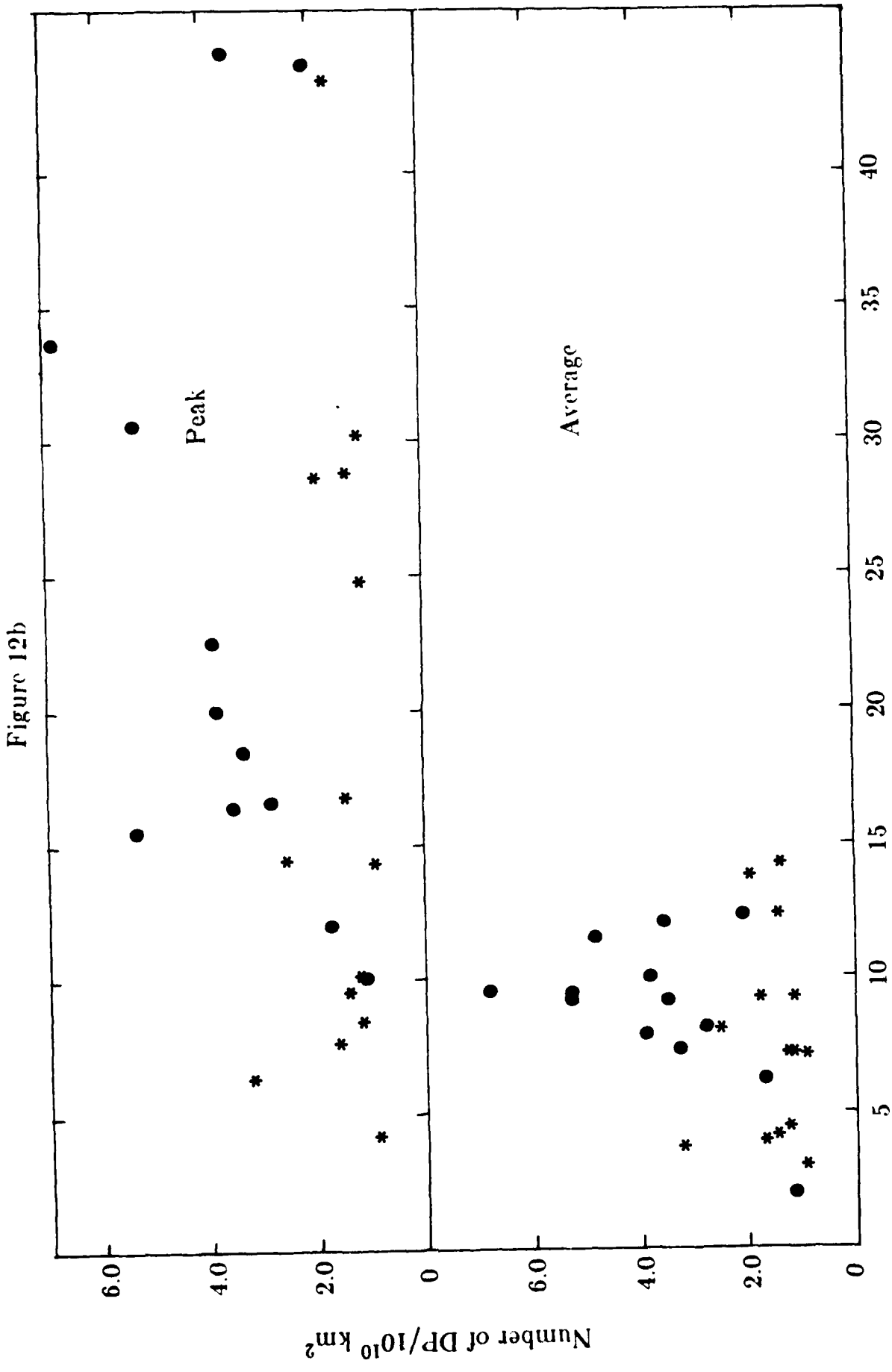
Peak
Average
6.0
4.0
2.0
0
5
10
15
20
25
30
35
40
Number of DP/10^{10} km^2
Ion Density of High Speed Solar Wind Streams (per cc)

Figure 12b

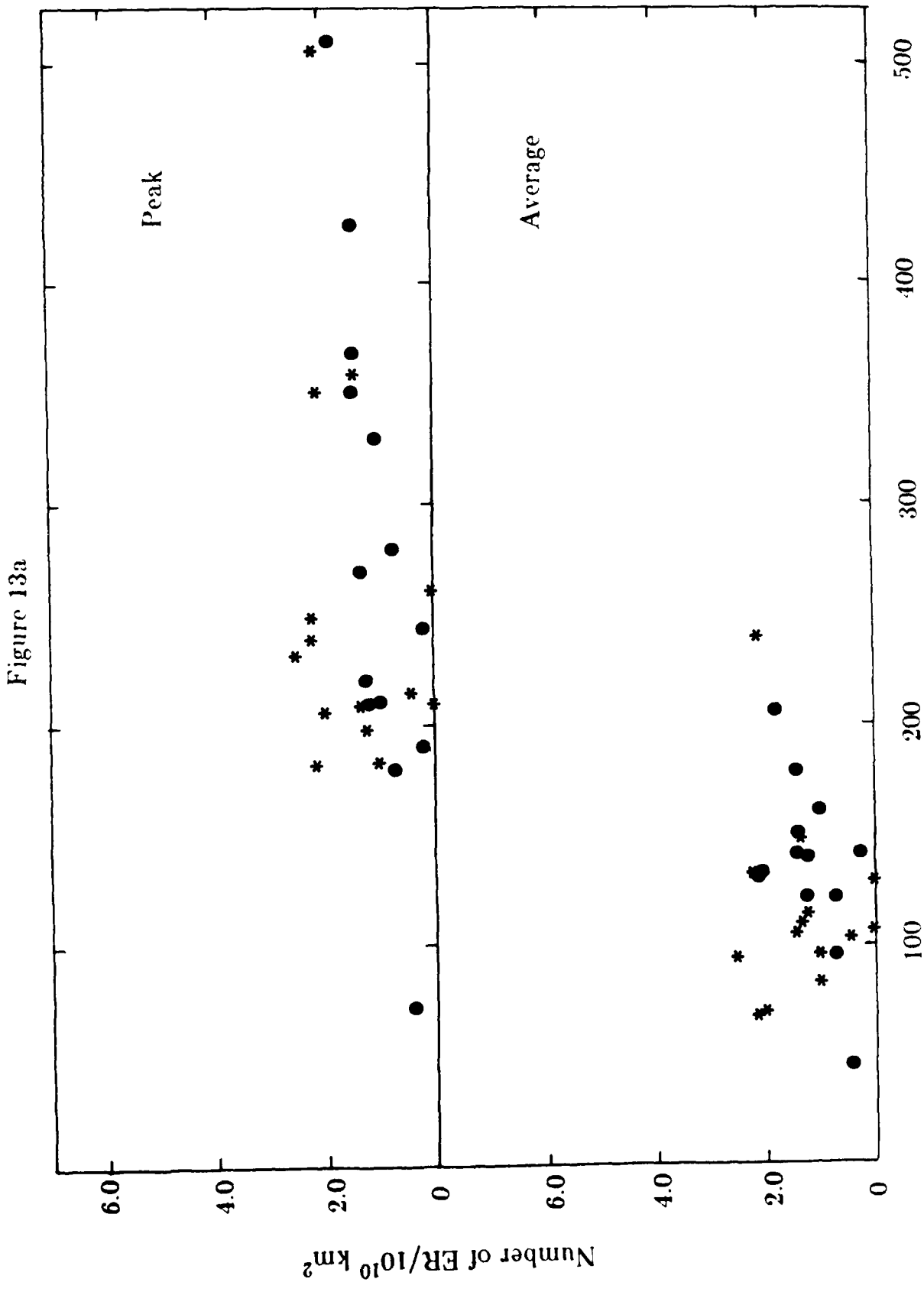
Peak
Average
Number of ER/10^10 km^2
6.0
4.0
2.0
0
100
200
300
400
500
Temperature of High Speed Solar Wind Streams (°K)

Figure 13a

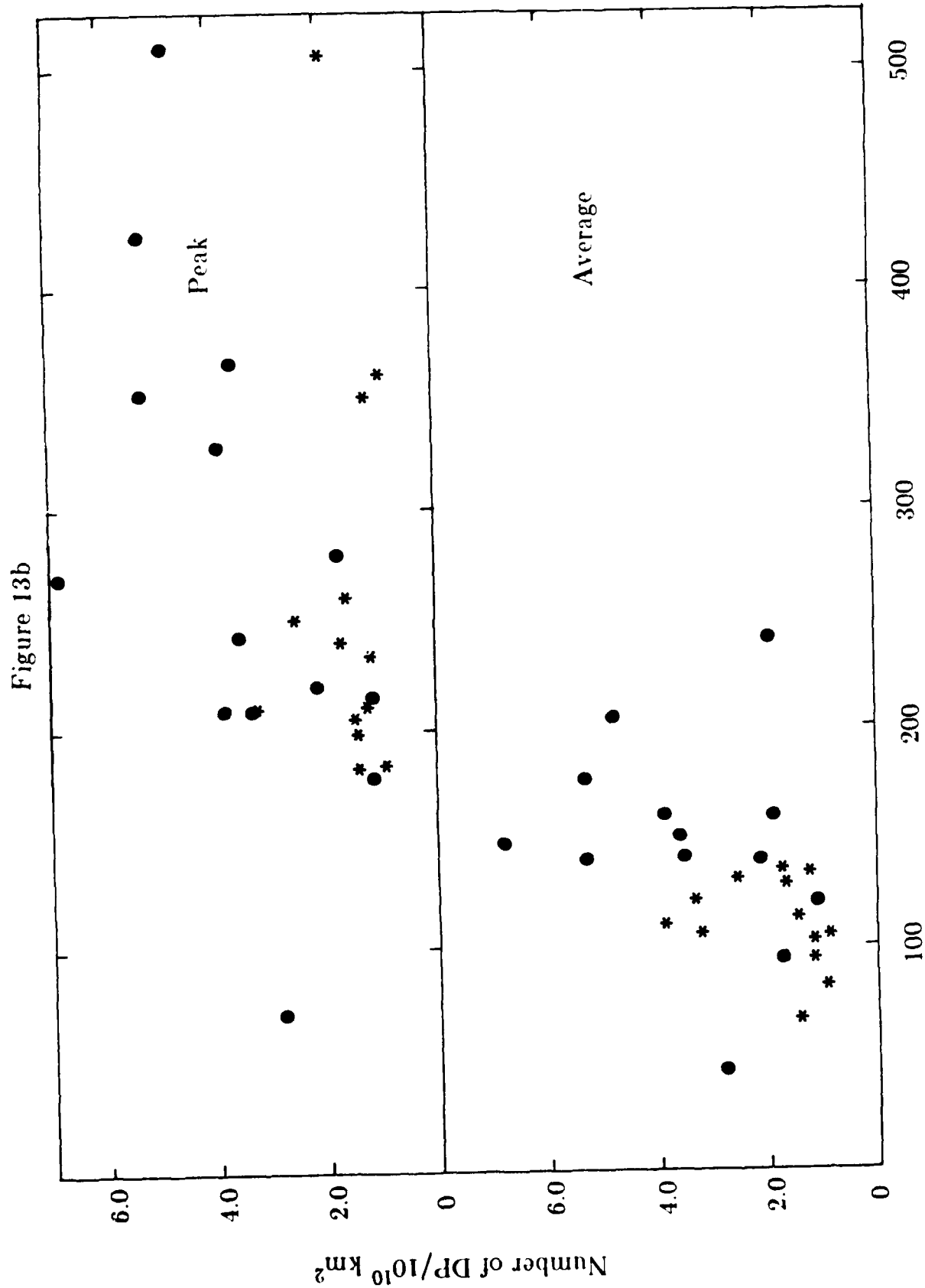
Peak
Average
Number of DP/10^{10} km^2
0
2.0
4.0
6.0
100
200
300
400
500
Temperature of High Speed Solar Wind Streams (° K)

Figure 13b

Figure 14

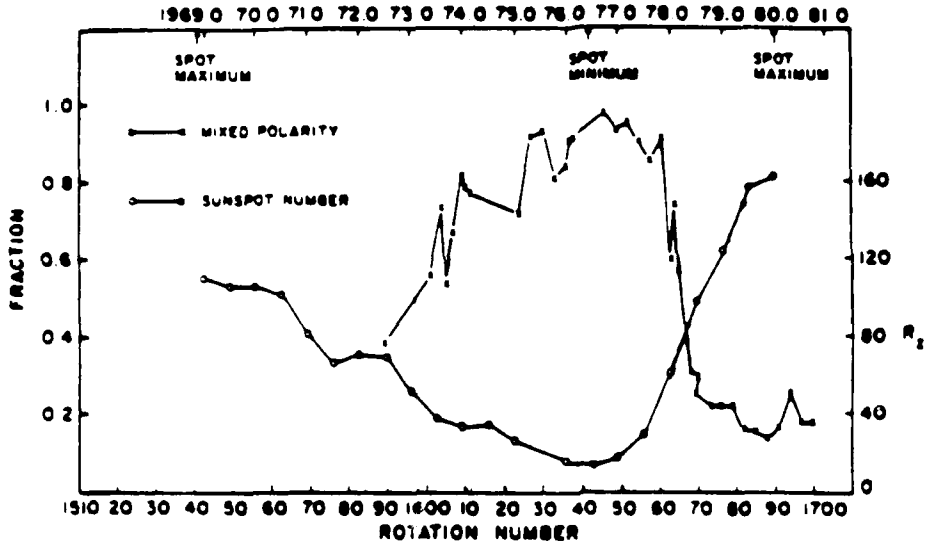
1969.0 70.0 71.0 72.0 73.0 74.0 75.0 76.0 77.0 78.0 79.0 80.0 81.0
SPOT MAXIMUM
SPOT MINIMUM
SPOT MAXIMUM
MIXED POLARITY
SUNSPOT NUMBER
FRACTION
1.0
0.8
0.6
0.4
0.2
160
120
80
40
0
R_z
1510 20 30 40 50 60 70 80 90 1600 10 20 30 40 50 60 70 80 90 1700
ROTATION NUMBER

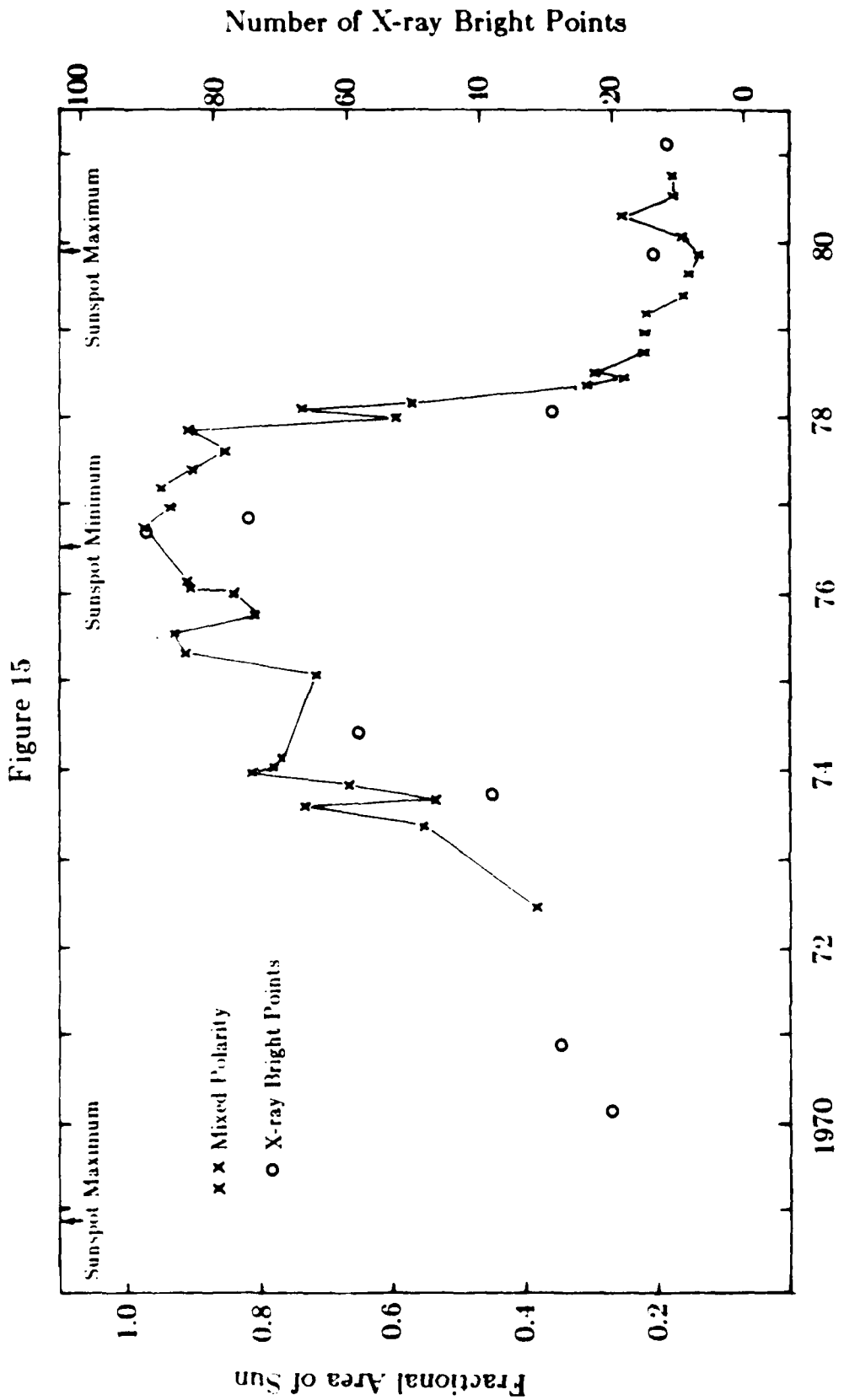
Number of X-ray Bright Points
100
80
60
40
20
0
Sunspot Maximum
Sunspot Minimum
Sunspot Maximum
Mixed Polarity
X-ray Bright Points
1.0
0.8
0.6
0.4
0.2
Fractional Area of Sun
1970
72
74
76
78
80

Figure 15

END

FILMED

7-85

DTIC